AN ACCURATE FREQUENCY ESTIMATION IN POWER NETWORKS IN THE PRESENCE OF HARMONICS

A THESIS SUBMITTED IN PARTIAL FULFILLMENT OF THE

REQUIREMENTS FOR THE DEGREE OF

Master of Technology

In

Electronics System and Communication Engineering

By

T. Purna Chandra Rao

Department of Electrical Engineering

National Institute of Technology

Rourkela

2007

AN ACCURATE FREQUENCY ESTIMATION IN POWER NETWORKS IN THE PRESENCE OF HARMONICS

A THESIS SUBMITTED IN PARTIAL FULFILLMENT OF THE

REQUIREMENTS FOR THE DEGREE OF

Master of Technology

In

Electronics System and Communication Engineering

By

T. Purna Chandra Rao

Under the Guidance of

Prof. P.C. Panda

Department of Electrical Engineering

National Institute of Technology

Rourkela

2007

National Institute of Technology

Rourkela

CERTIFICATE

This is to certify that the thesis entitled, **"An Accurate Frequency Estimation in Power networks in The presence of Harmonics"** submitted by Mr **T. Purna Chandra Rao** in partial fulfillment of the requirements for the award of MASTER of Technology Degree in **Electrical Engineering** with specialization in **"Electronics System and Communication Engineering"** at the National Institute of Technology, Rourkela (Deemed University) is an authentic work carried out by him/her under my/our supervision and guidance.

To the best of my knowledge, the matter embodied in the thesis has not been submitted to any other University/ Institute for the award of any degree or diploma.

Date:

Prof. P.C.Panda
Dept.of Electrical Engg.
National Institute of Technology
Rourkela - 769008

Acknowledgement

My sincere thanks to my guide **Prof.P.C.Panda** for his able guidance and constant support. I extend my thanks to our HOD, **Prof. P.K.Nanda** for his valuable advices, and to our PG-Coordinator **Prof. S.Ghosh** for his cooperation and encouragement, I also thank all the teaching and non-teaching staff for their cooperation to the students.

My special thanks to D.Pradeep Kumar and G V Rama krishna for their valuable suggestions and providing me good company in the lab. I also thank all my friends, without whose support my life might have been miserable here.

I wish to express my gratitude to my parents, whose love and encouragement have supported me throughout my education.

.

T. Purna Chandra Rao

CONTENTS

List of figures

List of tables

ABSTRACT

The main frequency is an important parameter of an electrical power system. The frequency can change over a small range due to generation-load mismatches. Some power system protection and control applications, e.g., frequency relay for load shedding, load-frequency controller, require accurate and fast estimation of the frequency. Most digital algorithms for measuring frequency have acceptable accuracy if voltage waveforms are not distorted. However, due to nonlinear devices, e.g., semiconductor rectifiers, electric arc furnaces, the voltage waveforms can include higher harmonics. The paper presents a new method of measurement of power system frequency, based on digital filtering and Prony's estimation method. Simulation results confirm, that the proposed method is more accurate than others, e.g., than the method based on the measurement of angular velocity of the rotating voltage phasor.

A precise digital algorithm based on Discrete Fourier Transforms (DFT) to estimate the frequency of a sinusoid with harmonics in real-time is proposed. This algorithm that we called the Smart Discrete Fourier Transforms (SDFT) smartly avoids the errors that arise when frequency deviates from the nominal frequency, and keeps all the advantages of the DFT e.g., immune to harmonics and the recursive computing can be used in SDFT. These make the SDFT more accurate than conventional DFT based techniques. In addition, this method is recursive and very easy to implement, so it is very suitable for use in real-time. We provide the simulation results compared with a conventional DFT method and second-order Prony method to validate the claimed benefits of SDFT.

Chapter 1

INTRODUCTION

1.1 BACKGROUND

With the progress of industry, power-electronic equipment is widely used in power systems, but the nonlinear characteristics of this equipment have also produced serious harmonic pollution. **F**requency is one of the most important quantities in power system operation because it can reflect the dynamic energy balance between load and generating power. So frequency is always regarded as an index of the operating practices, and utilities can know the system energy balance situations by observing frequency variations. Frequency may vary very fast in the transient events such that it is difficult to track it accurately. In addition, there are many devices, such as power electronic equipments and arc furnaces, etc. generating lots of harmonics and noise in modern power systems. It is therefore essential for utilities to seek and develop a reliable method that can measure frequency in presence of harmonics and noise. In addition, many ill effects (i.e., worse power quality for end users, more loss in transmission lines, overheating of machines, and malfunction of relays and breakers) are due to harmonic pollution. It goes without saying that "*harmonic analysis is a very important subject in power systems*".

1.2 OBJECTIVES

About harmonic analysis, several algorithms have been proposed and fast Fourier transform (FFT) is the most widely used computation algorithm for harmonic analysis. With the advent of the microprocessor, more and more microprocessor-based equipments have been extensively used in power systems. Using such equipments is known to provide accurate, fast responding, economic, and flexible solutions to measurement problems [1]. Therefore, all we have to do is to find the best algorithm and implement it. There have been many digital algorithms applied to estimating frequency during recent years, for example Modified Zero Crossing Technique [2], Level Crossing Technique [3], Least Squares Error Technique [4]–[6], Newton method [7], Kalman Filter [8]–[10], Prony Method [11], and Discrete Fourier Transform (DFT) [12], etc. About harmonic analysis, several algorithms have been proposed and Discrete Fourier transform (DFT) is the most widely used computation algorithm for harmonic analysis. However, leakage effect, less accuracy and low speed in presence of harmonics and noise, these effects make DFT suffer from specific restrictions. Therefore, some methods have also been provided to improve these drawbacks. For real-time use, most of the aforementioned methods have trade-off between accuracy and speed [13]. A precise digital algorithm, namely Smart Discrete Fourier Transform (SDFT) is presented and tries to meet the real-time use. SDFT has the advantages that it can obtain exact solution when

frequency deviates from nominal frequency, its speed is even faster than DFT, and it can get exact solution in the presence of harmonics.

1.3 Different techniques for frequency estimation:

- Least mean squares error techniques.
- NLMS technique.
- Adaptive combine filtering technique.
- Kalman filtering.
- Finite impulse response filtering.
- Zero crossing technique.
- Level crossing technique.
- FFT techniques.
- DFT techniques.
- Newton method.
- Prony method
- SDFT technique, etc

1.3.1Introduction

IN MANY power system protection and control schemes it is necessary to accurately measure and track the fundamental power frequency. In this paper specified three criteria that a frequency tracking method should satisfy in this application: i) fast speed of convergence; ii) accuracy of frequency estimation; and iii) robustness to noise. Other considerations are that, due to unbalanced loads or faults, it may be necessary to use just the information from one phase of a three phase supply and also the delay between the estimated frequency and the actual frequency may be important.

Six principle methods are compared in this paper and their ability to satisfy the requirements specified above are examined.

1.3.2: zero crossing methods:

This is a popular method in both protection and control. When using zero crossing methods, one determines the time between zero crossings of the signal to determine the frequency. This can be carried out by having a sliding window of *N* samples and curve fitting using a least squares technique. This method can be applied to a single phase, but three phases may be used together to provide the frequency at more intervals.

1.3.3: Quadratic Form:

This method is described in detail in Hacaoglu . Suppose that we are analyzing a set of signal samples defined by the vector $X = (x[n], x[n-1], ..., x[n-M+1])^T$. The quadratic form of X is defined as

$$F(x) = \sum_{m=0}^{M-1} \sum_{m=0}^{M-1} h[k,m]x[n-k]x[n-m] - - - - - (1.3.1)$$

Where $h[k,m]$ is the (k,m)th term of an $(M \times M)$ matrix, H . A nominal frequency of 50 Hz is assumed. In Reference .it is shown that, by taking the ratio of two quadratic forms of X with different matrices H_1 and H_2 that it is possible to obtain an approximate formula for the frequency.

1.3.4: Demodulation:

This procedure operates in analogy to demodulation of a Single Sideband Amplitude Modulated signal. Akke suggests that if three phases of the signal are available, then one can form two signals $V_\alpha[n]$ and $V_\beta[n]$ that are 90 out of phase by application of the $\alpha\beta$ Transform [4]. The complex signal is then formed from

$$V[n] = V_\alpha[n] + jV[n] = Ae^{j(\omega_1 t_n + \phi)} - - - - - (1.3.2).$$

Where ω_1 is the angular frequency at the th sample point and is the corresponding time of occurrence. In order to determine the frequency ω_1 , one demodulates $V[n]$ with the local oscillator term at angular frequency ω_0 . The frequency ω_1 can be found by differentiation of $\psi(n)$ with respect to time where $\psi(n) = (\omega_0 - \omega_0)t_n + \phi$.

One can apply demodulation with single phase data, but the filtering of a double frequency component is required which introduces a delay into the estimates ; the advantage of the complex demodulation method is that no such delay is introduce unless prefiteering of the data is carried out.

1.3.5: Discrete Fourier Transform with Phase Compensation

In this method, a DFT is computed over a 0.02 second segment of single phase data and the phase spectrum at 50 Hz is determined. By differentiation of this phase with respect to time, the frequency can be determined. In , this is extended to three phase data where the

positive sequence DFT is found. The frequency can be calculated using a batch least squares methods to fit a polynomial over a window of phase values.

1.3.6: Decomposition of Single Phase into Orthogonal Components

In the (DSPOC) method of Moore , which has been derived to analyze single phase data, the signal $s(t)$ is decomposed into two orthogonal components $x_1[t]$ and $x_2[t]$ as:

$$x_1[t] == \int_{-1/2T}^{1/2T} s(t-t')\sin(2\pi f_0 t')dt'$$

$$x_2[t] == \int_{-1/2T}^{1/2T} s(t-t')\cos(2\pi f_0 t')dt' \text{ -----(1.3.3).}$$

Where $T = 0.02$ s and f_0 is the reference frequency that is taken to be 50 Hz.

Each filter represents a band pass filter centered at 50 Hz, but which have phase responses that are $\pi/2$ out of phase.

The frequency is estimated from:

$$f_e(t) = 1/2\pi((x_2(t)\hat{x}_1(t) - x_1(t)\hat{x}_2(t))/(x^2{}_1(t) + x^2{}_2(t))) \text{ -----(1.3.4).}$$

One problem with this method is that the gains of the sine and cosine filters used in (4) are different away from the reference frequency of 50 Hz. This can be overcome by using an adaptive normalization procedure . The gains at the present estimated frequency are computed for the sine and cosine filters and this is used to renormalize the outputs x_1 and x_2.

1.3.7: Non-Linear Least Squares Estimation

Various authors have approached the problem of determining the frequency deviation from mains using estimation techniques.

The underlying signal is modeled by:

$$s(t) = A\cos(2\pi f_x t + \phi) \text{ -----(1.3.5).}$$

Which can be rewritten as:

$$s(t) = x_1\cos(2\pi(f_0 + f_1)t - x_2\cos(2\pi(f_0 + f_1)t \text{ -----(1.3.6).}$$

Where

x_1 is the in-phase component,

x_2 is the quadrature phase component,

f_0 is the reference frequency (50 Hz) and

f_1 is the frequency deviation.

Girgis *et al.* attempt a direct estimation of f_1 using Kalman filter techniques. The estimation problem here is nonlinear in that $s(t)$ is a nonlinear function of x_1, x_2 and f_1, hence the Extended Kalman Filter needs to be used. When x_3 has been estimated, this is further smoothed by being input into a linear Kalman filter; which assumes that the frequency changes according to a random ramp and random walk process. Kamwa and Grodin simplify this problem by rewriting:

$$s(t) = A\cos(2\pi f_0 t + \phi_1(t)) \text{-----} (1.3.7)$$

Recursive Least Squares (RLS) methods are applied to determine which is numerically differentiated $\phi_1(t)$ and smoothed to estimate of the frequency deviation from f_0.

1.3.8: Linear Estimation of Phase (LEP)

A novel approach follows on from the algorithm of Kamwa mentioned above but simplifies it to a *linear* estimation method to give amplitude and phase. Once the phase angle is known then the frequency can be estimated as it can be shown that the frequency error Δf is given by the time derivative of the phase.

The advantage of the LEP method is that, in theory, complete cycles of the sinusoid are not required in order to estimate the amplitude, frequency and phase. In practice the effects of noise mean that larger data segments than the theoretical minimum have to be used. The disadvantage of this method is that it can be adversely effected by nonsinusoidal components. However, the known harmonics can be simply removed or the signal has to be band pass filtered. For the types of power swing events studied here, it has been found that the nonfundamental components cannot be characterized as harmonics. A prefilter is therefore required so that the signal is dominated by the fundamental component. The prefilter used here is the FIR Hamming type filter as used.

Chapter 2

FREQUENCY ESTIMATION USING DFT ALGORITHM

2.1 FILTERED PHASORS FROM SAMPLED DATA

Consider a sinusoidal input signal of frequency ω given by

$x(t) = \sqrt{2}x\sin(\omega t + \phi)$ ----(2.1.1).

This signal is conventionally represented by a phasor (a complex number) X

$\hat{X} = Xe^{j\phi} = X\cos\phi + j\sin\phi$ ----(2.1.2).

Assuming that $x(t)$ is sampled N times per cycle of the 60 Hz waveform to produce the Sample set { x_K }

$x_K = \sqrt{2}x\sin(2\pi k / N + \phi)$ ----(2.1.3).

The Discrete Fourier Transform of { x_K } contains a fundamental frequency component given by

$$\hat{x}_1 = 2/N\sum_{k=0}^{N-1} x_k e^{-j2\pi k/N} \text{ ----(2.1.4).}$$

$$= 2/N\sum_{k=0}^{N-1} x_k \cos(2\pi k/N) - j2/N\sum_{k=0}^{N-1} x_k \sin(2\pi k/N)$$

$$= x_c - jx_s \text{ ----(2.1.5).}$$

where x_c and x_s are the cosine and sine multiplied sums in the expression for X1, Substituting for x_k from equation (2.1.3) in equations (2.1.4) and (2.1.5) it can be shown that for a sinusoidal input signal given by equation (2.1.1),

$x_c = \sqrt{2}x\sin\phi$

$x_s = \sqrt{2}x\cos\phi$ ----(2.1.6).

From equations (2.1.2), (2.1.5) and (2.1.6), it follows that the conventional phasor representation of a sinusoidal signal is related to the fundamental frequency component of its DFT By

$\hat{x} = 1/\sqrt{2}\, j\hat{x}_1 = 1/\sqrt{2}(x_s - jx_c)$ ----(2.1.7).

In the preceding development it was assumed that the input signal is a pure sine wave of fundamental frequency. When the input contains other frequency components as well, the phasor calculated by equation (2.1.7) is a filtered fundamental frequency phasor. The input signals must be band-limited to satisfy the Nyquist criterion to avoid errors due to aliasing effects. It is therefore assumed that the input signals are filtered with low-pass analog filters

having a cut-off frequency of wN/47 Hz. The effect of anti-aliasing analog filters on the fundamental frequency signals has been discussed in reference [14].

Another point to note is that equation (2.1.4) assumes data collected over one complete cycle of the fundamental frequency. Although the filter equations (2.1.4) are particularly simple for the case of a one cycle data window, similar filter equations can be formulated for any other window length. The consequence of using other window
Length is to affect the accuracy of the phasor computation. A more detailed discussion Of this aspect will be found in reference [15]. The remainder of this paper will assume the use of one cycle data window, it being a simple matter to modify one cycle data window results to reflect the effects of other data window lengths.

2.2 RECURSIVE PHASOR COMPUTATION

The input signal of equation (2.1.1) is shown in Figure (2.1). Data window 1 produces the sample set { $x(t)$, k=0, N-1} and the phasor representation obtained from this sample set is given by equation (2.1.7). A new sample is obtained after an elapsed (2.1.4) time corresponding to the sampling angle 27r/N radians. At this time the data window 2 becomes operative with sample set { x_k, k=l ..... The phasor computations using data window 2 are performed with
Equations (2.1.1), (2.1.2) and (2.1.7) as follows:

$$x(t) = \sqrt{2}x\sin(\omega t + \phi + 2\pi / N) ----(2.2.1).$$

$$\hat{x}^{(new)} = xe^{j(\phi+2\pi/N)} ----(2.2.2).$$

$$= \hat{x}^{(old)}e^{j2\pi/N}.$$

$$\hat{x}^{(new)} = 1/\sqrt{2}\, j\hat{x}_1^{(new)} ----(2.2.3).$$

$$= 1/\sqrt{2}(\hat{x}_s^{(new)} + j\hat{x}_c^{(new)}).$$

Where the superscripts 'new' and 'old' signify computations from data windows 2 and 1 respectively. Equation (2.2.2) shows that the use of equation (2.1.7) for calculating the filtered phasor of an input signal produces a phasor which rotates in a counterclockwise direction in the complex

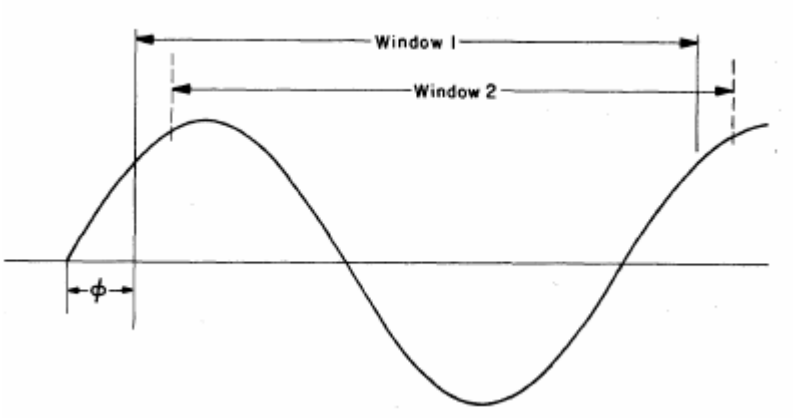

Figure: 2.1 data windows

Plane by the sampling angle 2w/N. This phenomenon is illustrated in Figure 2.2. The angular velocity of the phasor computed from a 60 Hz input signal is thus 120wf377 radians per second, although the phasor is available only at discrete angles.

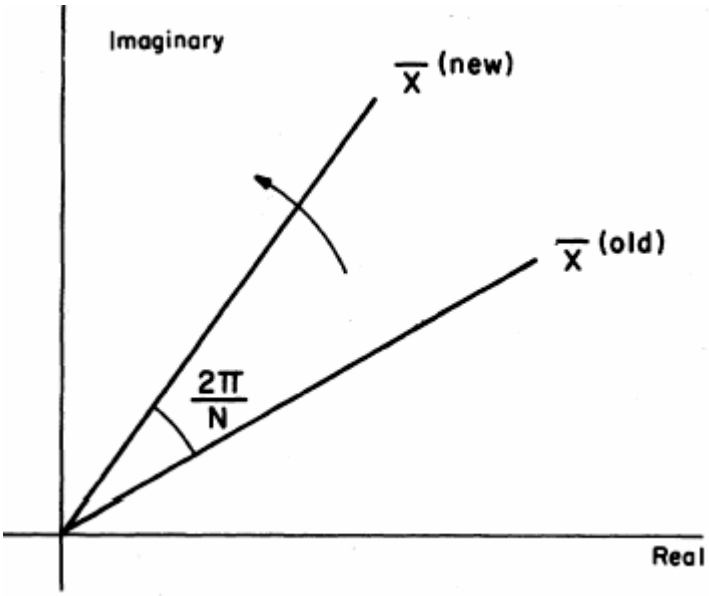

Figure: 2.2 phasors from different data windows.

$$x_c^{(r)} = 2/N \sum_{k=0}^{N-1} x_{k+r-1} \cos(2\pi k/N) ----(2.2.4).$$

$$x_s^{(r)} = 2/N \sum_{k=0}^{N-1} x_{k+r-1} \sin(2\pi k/N) ----(2.2.5).$$

$$\hat{x}^{(r)} = 1/\sqrt{2}(x_s{}^{(r)} + jx_c{}^{(r)})$$

$$= \hat{x}^{(r-1)} e^{j2\pi/N} ----(2.2.6).$$

Clearly the procedure described by (2.2.4)-(2.2.6) is non-recursive, and requires 2N multiplications an if (N-l) additions to produce the phasor X (The factor 2 is of no consequence, and is usually suppressed). It should however be noted that in progressing From one data window to the next, only one sample (x_o) is discarded and only one sample (x_N) is added to the data set. It is therefore advantageous to develop a technique which retains 2(N-1) multiplications and 2(N-1) sums corresponding to that portion of the data which is common to the old and new data windows.

A recursive computation of the type described above is made possible by the fact that the DFT computation is arbitrary to the extent of its phase angle. Consider the calculation of $x_c(\theta)$, $x_s(\theta)$ and $R(\theta)$ with Fourier coefficients having an arbitrary phase angle θ:

$$x_c{}^{(\theta)} = 2/N \sum_{k=0}^{N-1} x_{k+r-1} \cos(2\pi k/N + \theta) ----(2.2.7).$$

$$x_s{}^{(\theta)} = 2/N \sum_{k=0}^{N-1} x_{k+r-1} \sin(2\pi k/N + \theta) ----(2.2.8).$$

$$\hat{x}^{(\theta)} = \hat{x} e^{-j\theta} ----(2.2.9).$$

The phasor representation of the input signal in equation (2.2.9) contains as much information as does the one described by equations (2.1.2) and (2.1.7), and can therefore be used without any loss of generality. It is advantageous to calculate the phasor for data window 1 with equations (2.1.2) and (2.1.7), and that for data window 2 with equations (2.2.7) - (2.2.9):

If θ is now made equal to equations (2.2.7) and (2.2.8) become

$$x_c{}^{(new)}, 2\pi/N = x_c{}^{(old)} + 2/N \cos 2\pi(x_N - x_o) ----(2.2.10).$$

$$x_s{}^{(new)}, 2\pi/N = x_s{}^{(old)} + 2/N \sin 2\pi(x_N - x_o) ----(2.2.11).$$

If it is understood that the angle 0 is always set equal to 27r/N, this factor can be dropped From the superscript on the left hand side of equations (2.2.10) and (2.2.11), and the new Phasor is given by

$$\hat{x}^{(new)} = \hat{x}^{(old)} + j^{1/\sqrt{2}.2/N}(x_N - x_o)e^{-j2\pi/N} ----(2.2.12).$$

In general, the r^{th} phasor is computed from the (r-l)th phasor by

$$\hat{x}^{(r)} = \hat{x}^{(r-1)} + j^{1/\sqrt{2}.2/N}(x_{N+r} - x_r)e^{-j2\pi/N(r-1)} ----(2.2.13).$$

Recursive equations (2.2.10) and (2.2.11) are comparable to the non-recursive equations (2.2.4) and (2.2.5). With the recursive procedure only two multiplications need be performed at each new sample time; making this a very efficient computational algorithm.

It is interesting to note that when the input signal is a pure sine wave of fundamental frequency $X_{N+r} = X_r$ for all r; and consequently for this case equation (2.2.13) Becomes

$$\hat{x}^{(r)} = \hat{x}^{(r-1)} ----(2.2.14). \quad \text{for all r.}$$

Equation (2.2.14) shows that when a recursive computation is used to calculate phasors, it leads to stationary phasors in the complex plane when the input signal is a pure sine wave of fundamental frequency. Recall that non-recursive phasor computation leads to phasors which rotate in the complex plane: with an angular velocity w.

2.3 CALCULATION OF LOCAL FREQUENCY

Assume that the sampling clock used for obtaining the sampled data from the three phase voltage inputs operates precisely at 720 Hz while the power system frequency is precisely 60 Hz. When a recursive relation such as equation (2.2.13) is used to calculate the phasors, the resultant phasors will remain stationary in the complex plane. The equations derived in this section will consider phasor computations from a single input signal, although it may be verified readily that the results of this section apply directly to the positive sequence voltage calculated from three input voltage signals according to equation (2.2.14).

If the input signal frequency is now assumed to change slightly from 60 Hz by an amount &f, while the sampling clock frequency remains at 720 Hz, it can be shown that the recursive relation of equation (2.2.13) changes into

$$\hat{x}_{60+\Delta f}{}^{(r)} = \hat{x}_{60}{}^{(o)}(\sin(\Delta\pi f/60)/N\sin(\Delta\pi f/60N).e^{j(\Delta\pi f/60N)r}). ----(2.3.1).$$

Where X60 is the initial computation of the phasor from a 60 Hz input signal having the same magnitude as the $(60+\Delta f)$ Hz signal, r is the recursion number, and N is the number of samples in a period of the 60 Hz wave. Equation (2.3.1) shows that when the input signal Frequency changes from 60 Hz to $(60 + \Delta f)$ Hz, the phasor obtained recursively undergoes Two modifications:

A magnitude factor of $(\sin(\Delta f \pi / 60N))$; A f 27T and a phase factor of $e^{(j\Delta f 2\pi r/60N)}$. The magnitude factor is independent No f r, and is relatively small for small changes in frequency. The magnitude factor is a manifestation of the "leakage effect", and has been proposed as a measure of the frequency deviation Δf [2].

However, the phase angle effect is far more sensitive to the frequency Δf, and provides a most direct measure of Δf.

Denoting the phase factor by $\exp(j\psi r)$

$$e^{j(\Delta \pi f/60N)r} = e^{j\psi r} ----(2.3.2).$$

$$\psi_r = \Delta f / 60.2\pi / N.r ----(2.3.3).$$

And thus the phase angle at r^{th} recursive computation directly depends upon the frequency deviation and the recursion order r. Since r increases by 1 in each iteration,

The recursive relation for ψ_r becomes

$$\psi_r = \psi_{r-1} + \Delta f / 60.2\pi / N ----(2.3.4).$$

Further, the time interval between two iterations is 1/60N seconds: and therefore the angular velocity of p is given by

$$d\psi / dt = \psi_r - \psi_{r-1} /(1/60N). ----(2.3.5).$$

$2\pi \ \Delta f$ Radians/second.

The rate of change of the complex phasor angle is thus directly related to the input signal frequency. For example, an input signals with frequency (60 ± 1) Hz would produce a phasor that turns one complete circle per second in the complex plane. When the input signal frequency is 61 Hz, the phasor rotates in the counterclockwise direction, whereas for an input signal frequency of 59 Hz the phasor rotates in a clockwise direction. There is a striking resemblance between this phenomenon of a rotating phasor and the principle of a power system synchroscope so familiar to most power system engineers. Just as the frequency is calculated by calculating $d\psi / dt$ the rate of change of frequency can be calculated by computing $d^2\psi / dt^2$. From equation (2.3.5)

$$f = 60 + \Delta f$$

$$= 60 + 1/2\pi(d\psi / dt) hz ----(2.3.6).$$

$$df / dt = 1/2\pi(d^2\psi / dt^2) ----(2.3.7).$$

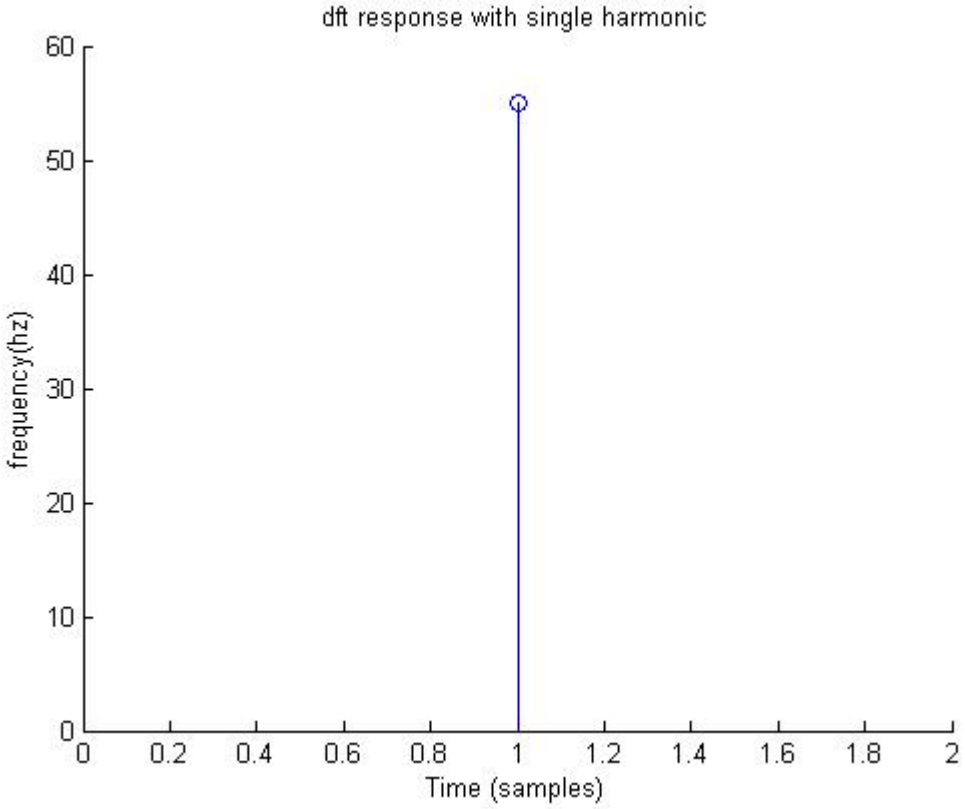

Figure 2.3: the estimated frequency component with single harmonic using DFT technique.

The actual computations for f and df / dt are performed with the help of regression formulas As explained below.

Chapter 3

PRONY METHOD

3.1 METHOD BASED ON THE DISCRETE FOURIER TRANSFORMATION

Some methods of frequency measurement, presented in literature during recent years base on the definition of the instantaneous frequency as angular velocity of the rotating voltage phasor. The phasor of the fundamental waveform of the voltage can be calculated from the N samples, using the DFT or other algorithms [16]–[20]. If the sampling window equals one cycle of the basic waveform, the phasor at the time $t_k = kT$ is given by

$$G_k = 2/N \sum_{n=0}^{N-1} v_{k+n-N+1} e^{-j\omega Tn} \text{----(3.1.1).}$$

Where:

T Sampling interval;

ω Fundamental frequency;

$v_{k+n-N+1}$ Sampled values of a voltage.

When implementing the method, G_k is updated at every sampled value. After each sampling cycle, the newest sample is taken into the calculation, while the oldest one is neglected. For each position of the phasor, its argument can be calculated. The instantaneous frequency can be determined from the two consecutive phasors.

$$\omega = \arg[G_{k+1}] - \arg[G_k]/T. \text{----(3.1.2).}$$

Where

$$\arg[G_k] = \tan^{-}\{\text{Im}[G_k]/\text{Re}[G_k]\}. \text{----(3.1.3).}$$

3.2 FILTERING

In the proposed approach a voltage waveform taken from a voltage transformer, is first filtered using algorithms based on the DFT. For further processing, we need only the time function of the fundamental component of voltage equals to the real part of the phasor. The filter algorithm is described as

$$g_k = 2/N \sum_{n=0}^{N-1} v_{k+n-N+1} \cos(n\omega T) \text{----(3.2.1).}$$

However, when the frequency changes, the rectangular window inherent in the DFT has some disadvantages. To improve the filter properties, applying of a smoothing window is
Proposed. The investigation was carried out for two most common window functions: Hamming window or Blackman window. The Hamming window is described by

$w_H = .54 - .46\cos(2\pi n / N - 1) - - - -(3.2.2).$

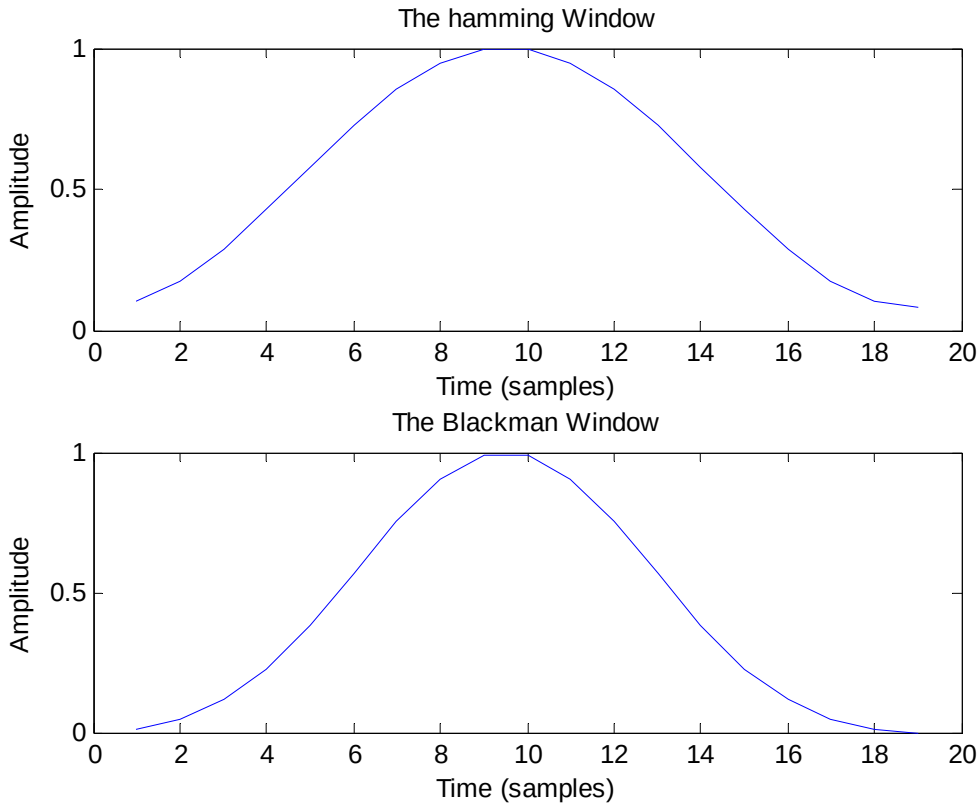

Figure 3.2.1: The amplitude response of hamming and Blackman window with N=20.

And the Blackman window described by

$w_B = .42 - .5\cos(2\pi n / N - 1) + .08\cos(4\pi n / N - 1) - - - -(3.2.3).$

The aim of the pre filtering is to improve the accuracy of the frequency determination.

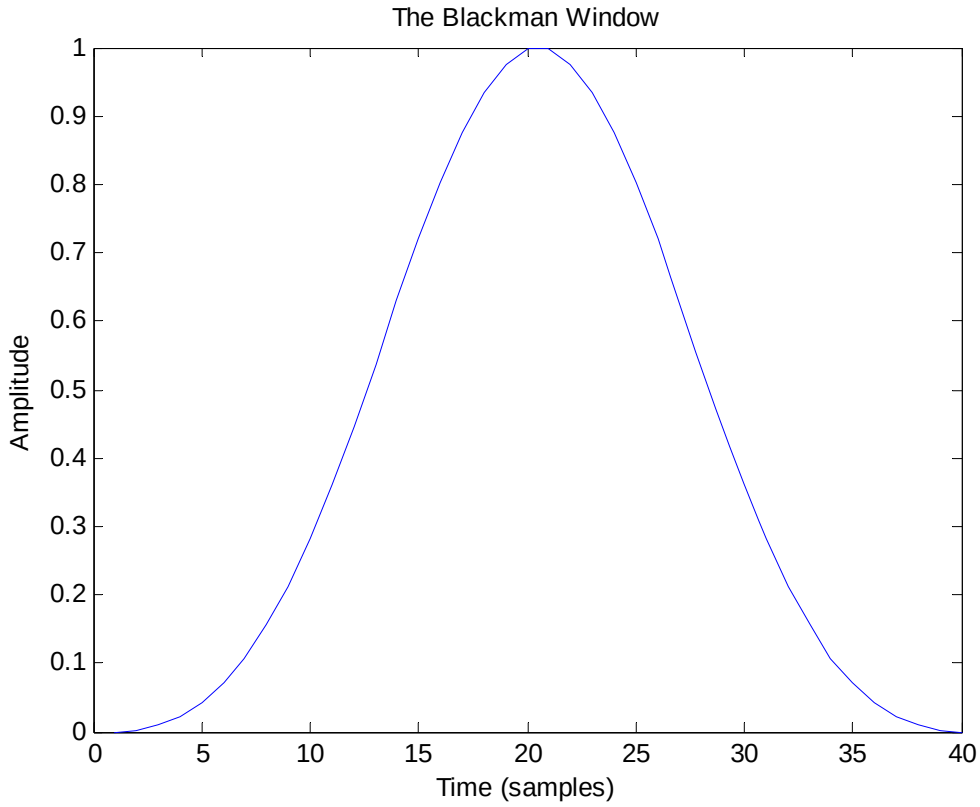

Figure 3.2.2: Blackman window with window size N=40.

3.3 ALGORITHM BASED ON THE PRONY'S ESTIMATON METHOD

At the output of the filter algorithm we obtain samples of the fundamental component of a voltage. Due to deviation of the frequency the filtering is not exact. For the calculation of the frequency we propose an algorithm based on the Prony's estimation method. The method is based on the assumption that given a series of samples g_1, g_2,.... g_M, a filtered voltage waveform can be approximated by one sinusoid

$y_m = A\cos(m\omega T + \psi)$ ----(3.3.1). From m=1,2,……..M.

Where M is the number of samples taken into the approximation. In the complex exponential form, this may be written as

$y_m = bz_1^m + bz_1^{*m}$ ----(3.3.2).

Where

$z_1 = e^{j\omega t}$ ----(3.3.3).

$b = A/2e^{j\psi}$ ----(3.3.4).

The estimation problem is, to find the values of b and z_1 so that the error

$\delta_m = g_m - y_m$ ----(3.3.5).

Will be minimized.

The key idea of the Prony's estimation method is to transform this nonlinear problem into a linear fitting problem by minimizing the error E defined as

$E = \sum_{m=p}^{M-1} (\varepsilon_m)^2$ ----(3.3.6).

Where p is the no of exponents and ε_m is defined by

$\varepsilon_m = \sum_{k=0}^{p} a_k \delta_{k+m-1}$ ----(3.3.7).

The parameters a_k are initially unknown, and are related to the frequency of the sinusoid. The key step to the estimation is to recognize that the (8) is the solution to some linear constant coefficient difference equation. In order to find the form of the difference equation, the polynomial $F(z)$ is defined for $p = 2$

$F(z) = a_0 (z - z_1)(z - z^*_1) = 0$ ----(3.3.8).

The exponents z_1 and z^*_1 are roots of the polynomial. Now, using (3.1.8) we obtain

$\sum_{k=0}^{2} a_k y_{k+m-1} = a_0 y_{m-1} + a_1 y_m + a_2 y_{m+1} = 0$ ----(3.3.9).

From (3.3.5) and (3.3.7) it follows that

$$\varepsilon_m = \sum_{k=0}^{2} a_k (g_{k+m-1} - y_{k+m-1})$$

$$= a_0 g_{m-1} + a_1 g_m + a_2 g_{m+1}$$ ----(3.3.10).

The desired roots z_1 of the polynomial $F(z)$ have unit modulus. If z_1 is a root, then z_1^{-1} is also. So the coefficients a_k are symmetric about a_1, i.e., $a_0 = a_2$. It is convenient to choose so that a_1=1. For $a_0 = a_2$, a_1=1.

$\varepsilon_m = g_m + a_0 (g_{m-1} + g_{m+1})$. ----(3.3.11).

The minimization of E with respect to the unknown a_0 will be achieved if

$\partial E / \partial a_0 = \sum_{m=2}^{M-1} 2[g_{m+} a_0 (g_{m-1} + g_{m+1})](g_{m-1} + g_{m+1}) = 0$ ----(3.3.12).

A solution of (3.3.12) we obtain

$$a_0 = -\sum_{m=2}^{M-1} g_m a_0 (g_{m-1} + g_{m+1}) / \sum_{m=2}^{M-1} g_m a_0 (g_{m-1} + g_{m+1})^2 \text{ ----(3.3.13).}$$

The polynomial $F(z)$ (3.1.14) can be expressed as

$$z^2 + (1/a_0)z + 1 = 0 \text{ ----(3.3.14).}$$

The roots of polynomial are

$$z_{1,2} = -1/2a_0 \pm j\sqrt{1-1/4a^2{}_0} \text{ ----(3.3.15).}$$

Since the roots are defined as (3.3.2)

$$z_{1,2} = e^{\pm j\omega T}$$

$$= \cos(\omega T) \pm j \sin(\omega T). \text{ ----(3.3.16).}$$

The angular frequency ω is given by

$$\omega = 1/T \cos^{-1}\{\sum_{m=2}^{M-1} (g_{m-1} + g_{m+1})^2 / 2 \sum_{m=2}^{M-1} g_m (g_{m-1} + g_{m+1})\}. \text{ ----(3.3.17).}$$

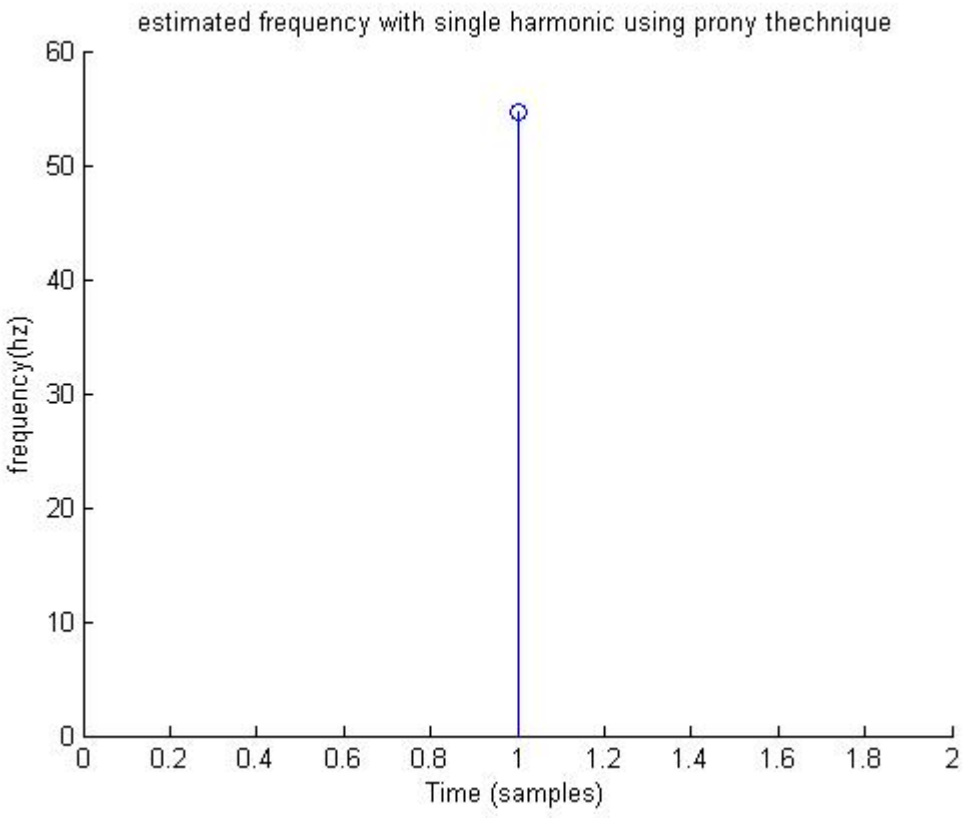

Figure 3.3.1: frequency response with single harmonic using prony technique

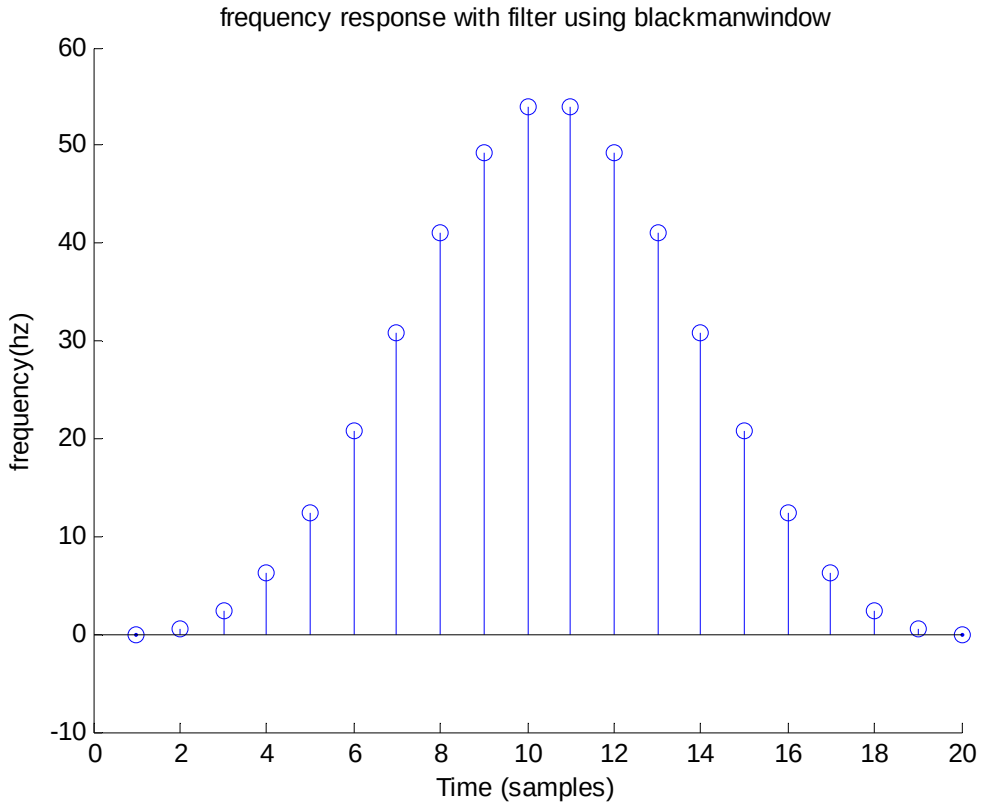

Figure 3.3.2: frequency response with filter with multiple harmonics

3.4 SIMULATION RESULTS

The developed method was investigated on computer and compared to the method based on the DFT. The program generates a voltage which is sampled at preselected rate. These samples were processed according to (3.1.1) to calculate the phasor, and according to (3.1.4) to calculate the time function of the main waveforms. The frequency was calculated either Using the (3.1.2) or using the new method, described by (3.3.17). The voltage waveforms were distorted by higher harmonics.

When implementing the methods, the calculated frequency is updated at every sampled value: After each sampling cycle, the newest sample is taken into the calculation, while the oldest one is neglected.

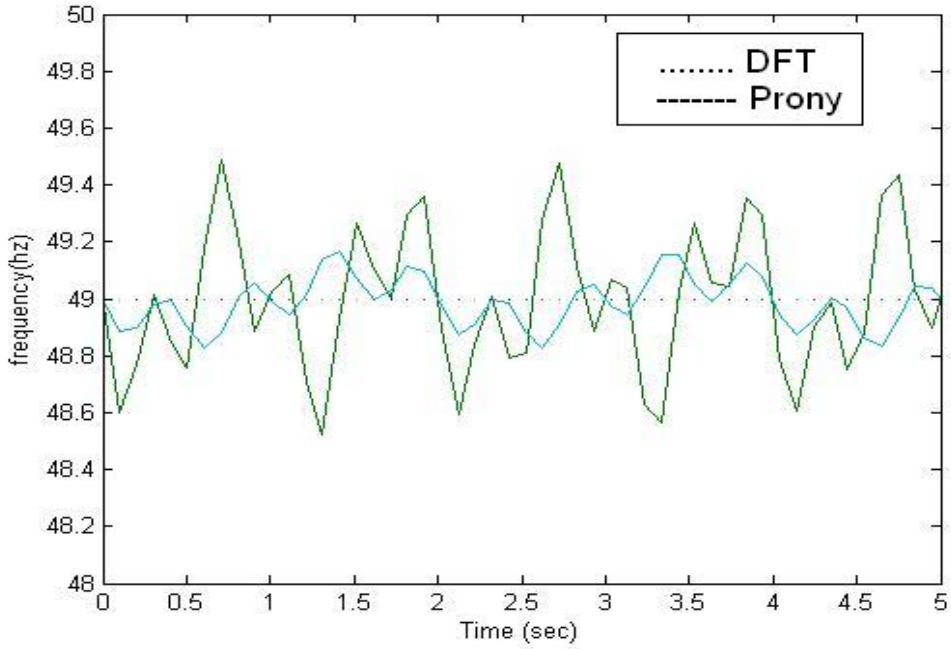

Figure 3.4.1: Estimated frequency of a voltage $g(t) = \cos(\omega t) + .2\cos(5\omega t) + .1\cos(7\omega t)$; simulated frequency f =49 Hz, sampling frequency f_s =1000 Hz, filter order N=20, M-number of samples of the prony's model, M=15.

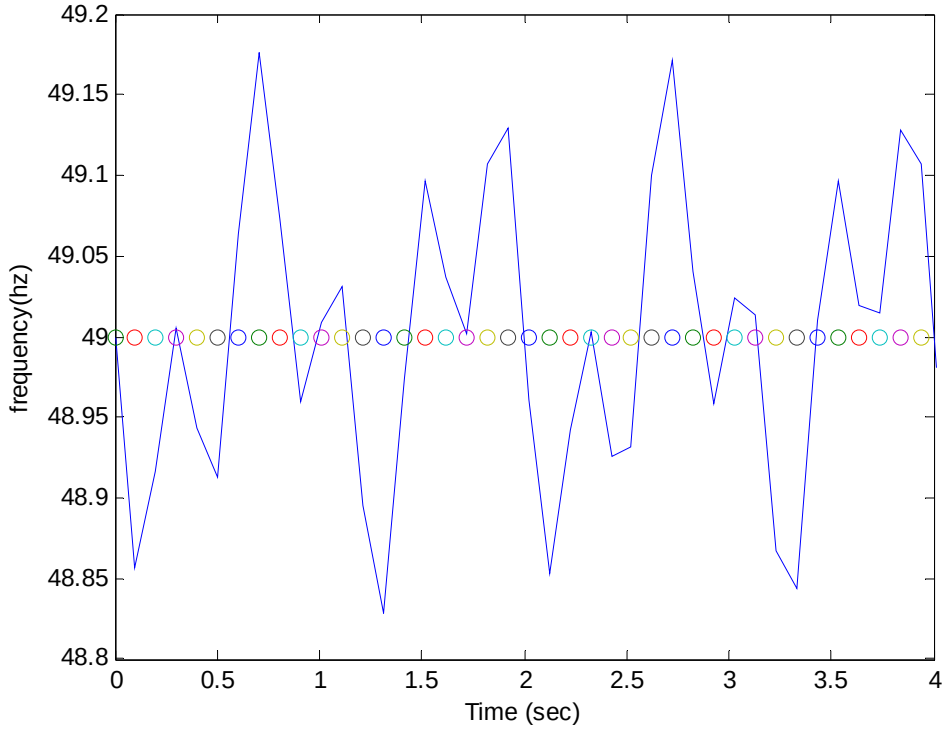

Figure3.4.2:Estimated frequency of a voltage $g(t) = \cos(\omega t) + .2\cos(5\omega t) + .1\cos(7\omega t)$; simulated frequency f =49 Hz, sampling frequency f_s =1000 Hz, filter order N=20, M-number of samples of the prony's model, M=20.

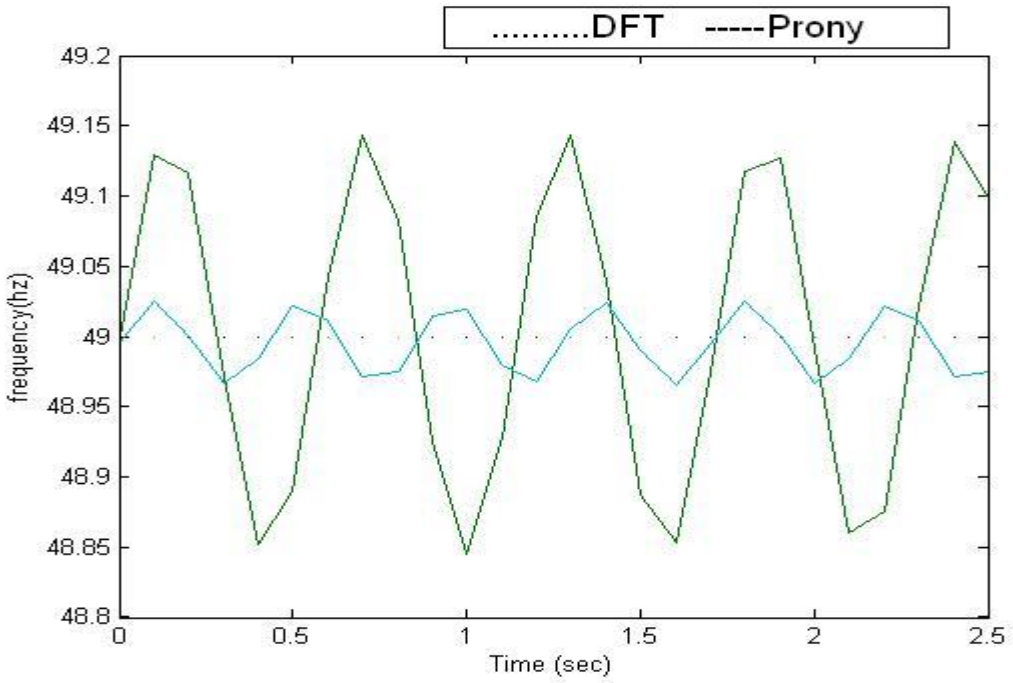

Figure3.4.3:estimated frequency of a voltage $g(t) = \cos(\omega t) + .2\cos(5\omega t) + .1\cos(7\omega t)$; **simulated frequency** f **=49 Hz, sampling frequency** f_s **=1000 Hz, filter order N=40, M-number of samples of the prony's model, M=15.**

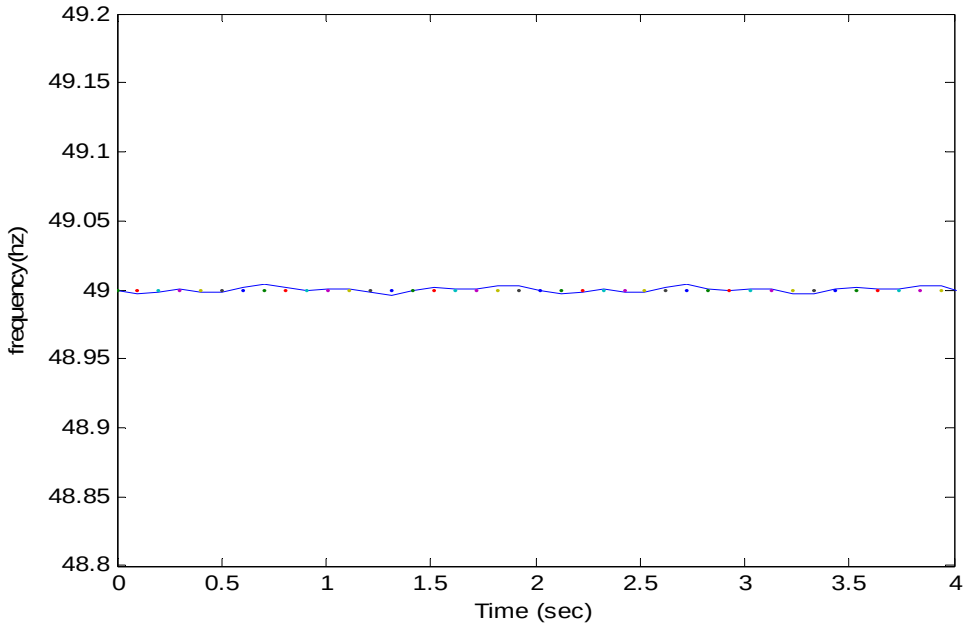

Figure3.4.4: Estimated frequency of a voltage $g(t) = \cos(\omega t) + .2\cos(5\omega t) + .1\cos(7\omega t)$; **simulated frequency** f **=49 Hz, sampling frequency** f_s **=1000 Hz, filter order N=40, M-number of samples of the prony's model, M=20.**

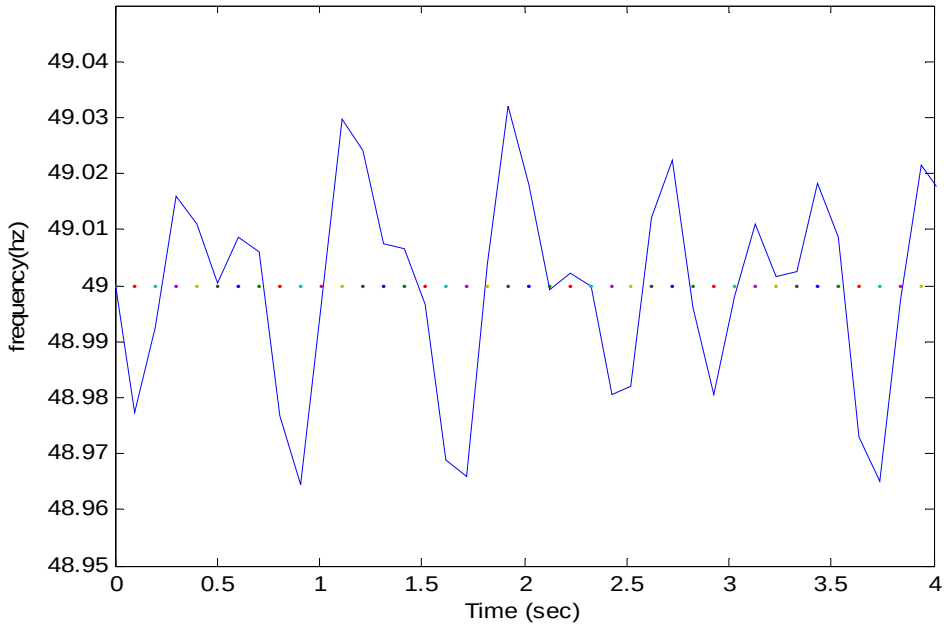

Figure3.4.5: estimated frequency of a voltage $g(t) = \cos(\omega t) + .2\cos(5\omega t) + .1\cos(7\omega t)$; simulated frequency f =49 Hz, sampling frequency f_s =1000 Hz, filter order N=40, M-number of samples of the prony's model, M=5.

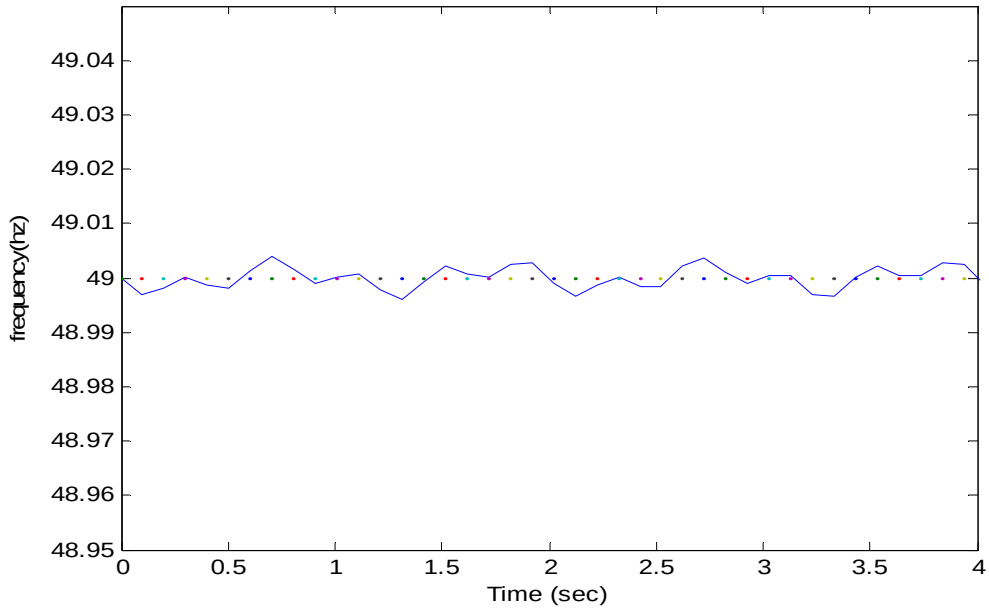

Figure3.4.6: estimated frequency of a voltage $g(t) = \cos(\omega t) + .2\cos(5\omega t) + .1\cos(7\omega t)$; simulated frequency f =49 Hz, sampling frequency f_s =1000 Hz, filter order N=40, M-number of samples of the prony's model, M=30.

Fig.3.4. shows results of frequency estimation for heavy distorted voltage waveform $g(t) = \cos(\omega t) + .2\cos(5\omega t) + .1\cos(7\omega t)$. Fig. 3.4.1 shows results when applying the Hamming window, Fig. 3.4.2 and 3.4.3 the Blackman window. For comparison, the results when applying the DFT method have also been shown. The best accuracy has been achieved using the Blackman smoothing window.

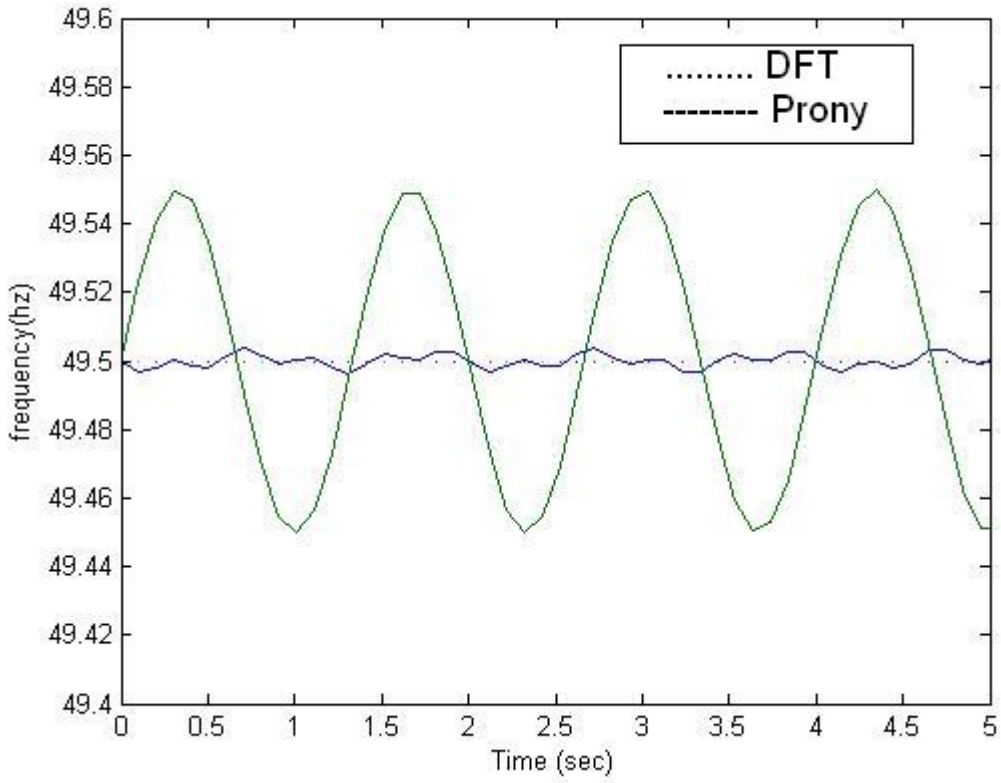

Figure3.4.7: estimated frequency of a voltage $g(t) = \cos(\omega t) + .02\cos(5\omega t) + .01\cos(7\omega t)$; simulated frequency f =49.5 Hz, sampling frequency f_s =1000 Hz, filter order N=20, M-number of samples of the prony's model, M=15.

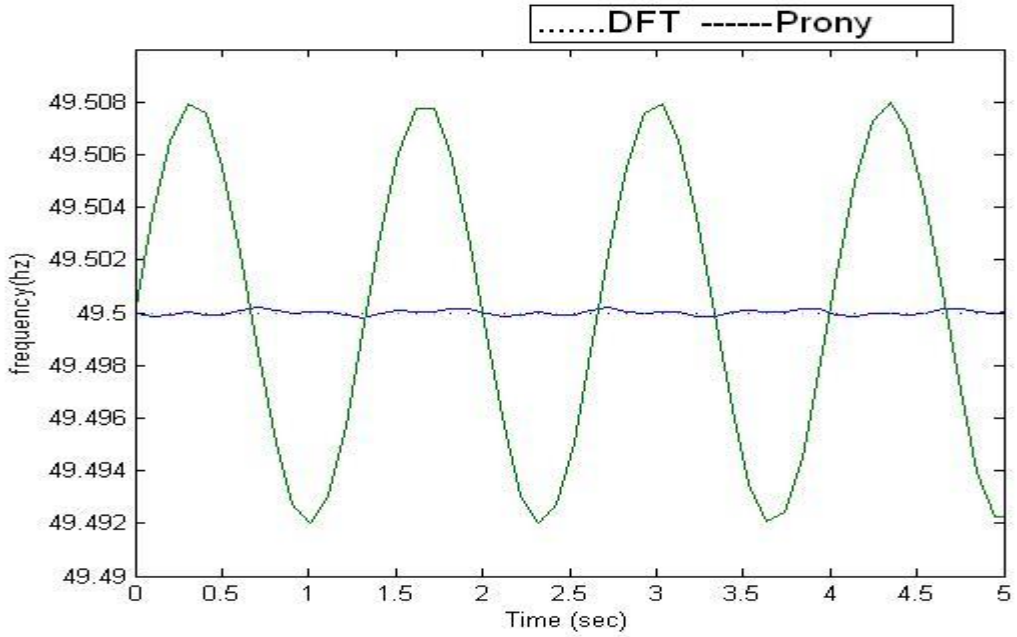

Figure3.4.8: estimated frequency of a voltage $g(t) = \cos(\omega t) + .02\cos(5\omega t) + .01\cos(7\omega t)$; **simulated frequency** f **=49.5 Hz, sampling frequency** f_s **=1000 Hz, filter order N=40, M-number of samples of the prony's model, M=15.**

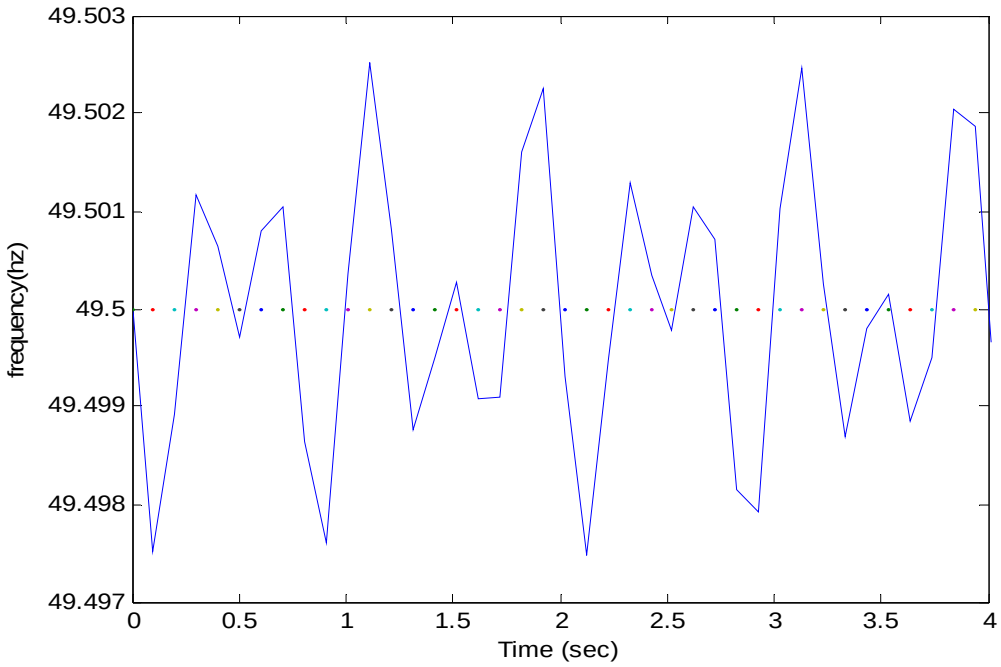

Figure3.4.9: estimated frequency of a voltage $g(t) = \cos(\omega t) + .02\cos(5\omega t) + .01\cos(7\omega t)$; **simulated frequency** f **=49.5 Hz, sampling frequency** f_s **=1000 Hz, filter order N=40, M-number of samples of the prony's model, M=5.**

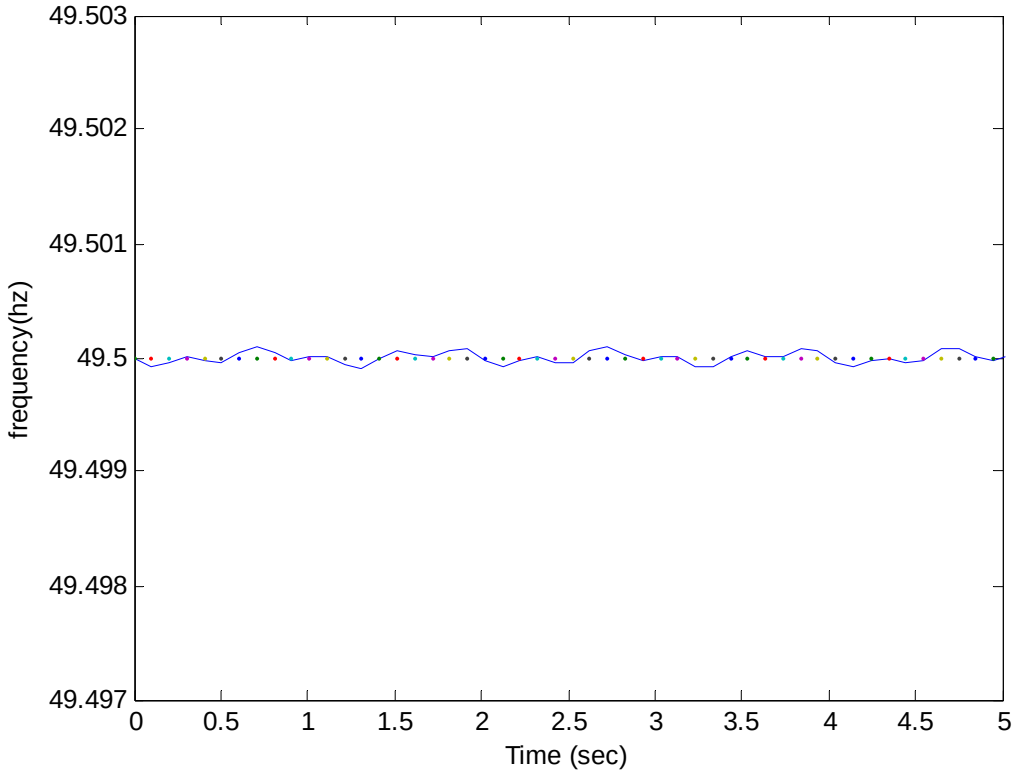

Figure3.4.10: estimated frequency of a voltage $g(t) = \cos(\omega t) + .02\cos(5\omega t) + .01\cos(7\omega t)$; **simulated frequency** f **=49.5 Hz, sampling frequency** f_s **=1000 Hz, filter order N=40, M-number of samples of the prony's model, M=30.**

Fig. 3.4.7 shows results for the voltage waveform with realistic distortion in high voltage networks $g(t) = \cos(\omega t) + .02\cos(5\omega t) + .01\cos(7\omega t)$. The computer investigation disclosed a high accuracy of the developed method. For realistic voltage distortion and frequency deviation the error was less than 1 mHz. The dynamic behavior of the method was also investigated. The results showed in Fig. 3.4.11 confirm a good tracking capability of the method.

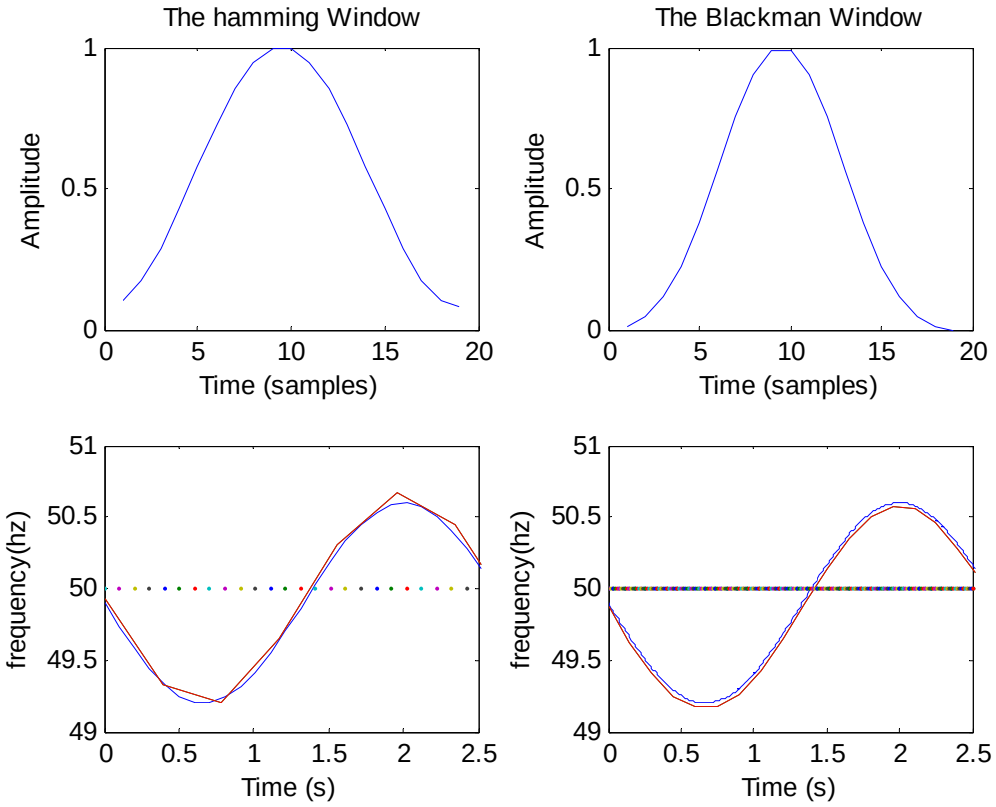

Figure3.4.11:True and estimated frequency of a voltage

$g(t) = \cos(\omega t) + .2\cos(5\omega t) + .1\cos(7\omega t);$ **with sampling frequency** f_s **=1000 Hz, filter** order **N=20, M- no of samples M=30.**

Chapter 4

THE PROPOSED DIGITAL ALGORITHM

4.1 The proposed digital algorithm

This section presents the algorithm of the SDFT that calculates the frequency from a voltage/current signal. Consider a sinusoidal input signal of frequency $\omega = 2\pi f$ with mth harmonic given by

$$x(t) = X_1 \cos(\omega t + \phi_1) + X_2 \cos(m\omega t + \phi_2) ----(4.1.1)$$

Where

X_1, X_2: the amplitude,

ϕ_1, ϕ_2: the phase angle,

Suppose that $x(t)$ is sampled with a sampling rate (60*N) Hz waveform to produce the sample set $\{x(k)\}$

$$x(k) = X_1 \cos(\omega k / 60N + \phi_1) + X_2 \cos(m\omega k / 60N + \phi_2) ----(4.1.2)$$

The signal $x(t)$ is conventionally represented by a phasor (a complex number)

$$= Xe^{j\phi} = X\cos\phi + jX\sin\phi. ----(4.1.3).$$

The $x(t)$ can be expressed as

$$x(t) = e^{j\omega t} + e^{-j\omega t} / 2 + e^{jm\omega t} + e^{-jm\omega t} / 2. ----(4.1.4).$$

Where denotes complex conjugate. Moreover, the fundamental frequency (60 Hz) component of DFT of $\{x(k)\}$ is given by

$$\hat{x}_r = 2 / N \sum_{k=0}^{N-1} x(k+r) \exp(-j2\pi k / N). ----(4.1.5).$$

Combing (4.1.4) and (4.1.5) and taking frequency deviation [$\omega = 2\pi(60 + \Delta f)$] into consideration,

we obtain:

$$\hat{x}_r = / N \sum_{k=0}^{N-1} \exp(j2\pi(60+\Delta f)(k+r)/60N).\exp(-j2\pi k/N)$$
$$+ / N \sum_{k=0}^{N-1} \exp(-j2\pi(60+\Delta f)(k+r)/60N).\exp(-j2\pi k/N)$$
$$+ / N \sum_{k=0}^{N-1} \exp(j2\pi(60+\Delta f)m(k+r)/60N).\exp(-j2\pi k/N)$$
$$+ / N \sum_{k=0}^{N-1} \exp(-j2\pi(60+\Delta f)m(k+r)/60N).\exp(-j2\pi k/N) ----(4.1.6)$$

We rearrange (4.1.6) as the following

$$X(r) = \alpha_1 / N \exp(j2\pi / N(1+\Delta f / 60)r)\sum_{k=0}^{N-1}\exp(j2\pi(\Delta f / 60N)k)$$

$$+\alpha_1^* / N \exp(-j2\pi / N(1+\Delta f / 60)r)\sum_{k=0}^{N-1}\exp(-j2\pi(2+\Delta f / 60N)k)$$

$$+\alpha_2 / N \exp(j2\pi / N(1+\Delta f / 60)mr)\sum_{k=0}^{N-1}\exp(j2\pi(m-1+m\Delta f / 60N)k)$$

$$+\alpha_2^* / N \exp(-j2\pi / N(1+\Delta f / 60)mr)\sum_{k=0}^{N-1}\exp(-j2\pi(-1-m+m\Delta f / 60N)k) ----(4.1.7)$$

We use the following identity to simplify (4.1.7).

$$\sum_{i=0}^{N-1}(e^{j\theta})^i = \sin(N\theta/2)/\sin(\theta/2)\exp(j(N-1)\theta/2). ----(4.1.8).$$

Then (4.1.7) can be expressed as

$$X(r) = \alpha_1 / N \exp(j2\pi / N(1+\Delta f / 60)r)\sin(N\theta_1/2)/\sin(\theta_1/2).\exp(j(N-1)\theta_1/2)$$
$$+\alpha_1^* / N \exp(-j2\pi / N(1+\Delta f / 60)r)\sin(N\theta_2/2)/\sin(\theta_2/2).\exp(j(N-1)\theta_2/2)$$
$$+\alpha_2 / N \exp(j2\pi / N(1+\Delta f / 60)mr)\sin(N\theta_3/2)/\sin(\theta_3/2).\exp(j(N-1)\theta_3/2)$$
$$+\alpha_2^* / N \exp(-j2\pi / N(1+\Delta f / 60)mr)\sin(N\theta_4/2)/\sin(\theta_4/2).\exp(j(N-1)\theta_4/2). ----(4.1.9)$$

Where

$\theta_1 = 2\pi(\Delta f / 60N)$,

$\theta_2 = -2\pi(2+\Delta f / 60N)$,

$\theta_3 = 2\pi(m-1+m\Delta f / 60N)$,

$\theta_4 = 2\pi(-m-1+m\Delta f / 60N)$.

Rearranging (4.1.9) further we obtain

$$X(r) = \alpha_1 / N \sin(N\theta_1/2)/\sin(\theta_1/2)\exp(j\pi/60N(\Delta f(2r+N-1+120r))$$
$$+\alpha_1^* / N \sin(N\theta_2/2)/\sin(\theta_2/2)\exp(-j\pi/60N(\Delta f(2r+N-1+120(r+N-1)))$$
$$+\alpha_2 / N \sin(N\theta_3/2)/\sin(\theta_3/2)\exp(j\pi/60N(m\Delta f(2r+N-1+60(2mr+mN-m-N+1)))$$
$$+\alpha_2^* / N \sin(N\theta_4/2)/\sin(\theta_4/2)\exp(-j\pi/60N(m\Delta f(2r+N-1+60(2mr+mN-m-N-1))). ----(4.1.10)$$

If we define A_r, B_r, C_r and D_r as

$A_r = \alpha_1 / N \sin(N\theta_1/2)/\sin(\theta_1/2)\exp(j\pi/60N(\Delta f(2r+N-1+120r))$

$B_r = \alpha_1^* / N \sin(N\theta_2/2)/\sin(\theta_2/2)\exp(-j\pi/60N(\Delta f(2r+N-1+120(r+N-1)))$

$C_r = \alpha_2 / N \sin(N\theta_3/2)/\sin(\theta_3/2)\exp(j\pi/60N(m\Delta f(2r+N-1+60(2mr+mN-m-N+1)))$

$D_r = \alpha_2^* / N \sin(N\theta_4/2)/\sin(\theta_4/2)\mathrm{e}(-j\pi/60N(m\Delta f(2r+N-1+60(2mr+mN-m-N-1)))$.

Then (4.1.9) can be expressed as

$\hat{x}_r = A_r + B_r + C_r + D_r$.-----(4.1.11).

Except the parts of m^{th} harmonic, so far the development of the algorithm of SDFT are the same as the conventional DFT method. So the SDFT can keep all advantages of DFT such as Recursive computing manner. But in the DFT, it assumes that the frequency deviation is small enough to be ignored, and it always considers $\hat{x}_r = A_r$, so traditional DFT based methods incur error in estimating frequency and phasor when frequency deviates from nominal frequency (60 Hz). If we want to get exact solution, we must take B_r , C_r and D_r into consideration.

So we define

$a = \exp(j(\pi / 60N(2\Delta f + 120)))$.----(4.1.12).

And from (4.1.10), we will find the following relations

$A_{r+1} = A_r a$ ----(4.1.13).

$B_{r+1} = B_r a^{-1}$ ----(4.1.14).

$C_{r+1} = C_r a^m$ ----(4.1.15).

$D_{r+1} = D_r a^{-m}$ ----(4.1.16).

Then

$\hat{x}_{r+1} = A_r a + B_r a^{-1} + C_r a^m + D_r a^{-m}$ ----(4.1.17).

$\hat{x}_{r+2} = A_{r+1} a + B_{r+1} a^{-1} + C_{r+1} a^m + D_{r+1} a^{-m}$ ----(4.1.18).

If we multiplied "a^m" both sides (4.1.17) and (4.1.18) respectively, then we get,

$a^m \hat{x}_{r+1} = A_r a^{1+m} + B_r a^{-1+m} + C_r a^{2m} + D_r$ ----(4.1.19).

$a^m \hat{x}_{r+2} = A_{r+1} a^{1+m} + B_{r+1} a^{-1+m} + C_{r+1} a^{2m} + D_{r+1}$ ----(4.1.20).

Subtracting (4.1.11) from (4.1.19) and subtracting (4.1.17) from (4.1.20), respectively, we can erase D_r and obtain

$\hat{y}_r = a^m \hat{x}_{r+1} - \hat{x}_r$

$= A_r (a^{1+m} - 1) + B_r (a^{-1+m} - 1) + C_r (a^{2m} - 1)$ ----(4.1.21).

$\hat{y}_{r+1} = a^m \hat{x}_{r+2} - \hat{x}_{r+1}$

$= A_{r+1} (a^{1+m} - 1) + B_{r+1} (a^{-1+m} - 1) + C_{r+1} (a^{2m} - 1)$ ----(4.1.22).

Repeat similar operation to erase the B_r and C_r, then the equations will become

$$a\hat{Z}_{r+1} - \hat{Z}_r = A_r(a^2 - 1)(a^{1-m} - 1)(a^{1+m} - 1) ----(4.1.23).$$

$$a\hat{Z}_{r+2} - \hat{Z}_{r+1} = A_{r+1}(a^2 - 1)(a^{1-m} - 1)(a^{1+m} - 1) ----(4.1.24).$$

Where $\hat{Z}_r = a\hat{u}_{r+1} - \hat{u}_r, \quad \hat{u}_r = a^{-m}\hat{y}_{r+1} - \hat{y}_{r.}$

Dividing (4.1.24) by (4.1.23), we get

$$a\hat{Z}_{r+2} - \hat{Z}_{r+1} / a\hat{Z}_{r+1} - \hat{Z}_r = A_{r+1} / A_r = a. ----(4.1.25).$$

Then expand (4.1.25), and use numerical method to find the solution of "a ." And from the definition of "a " in (4.1.12), we can get the exact solution of the frequency.

$$f = 60 + \Delta f = \cos^{-1}(Re(a))60N / 2\pi. ----(4.1.26).$$

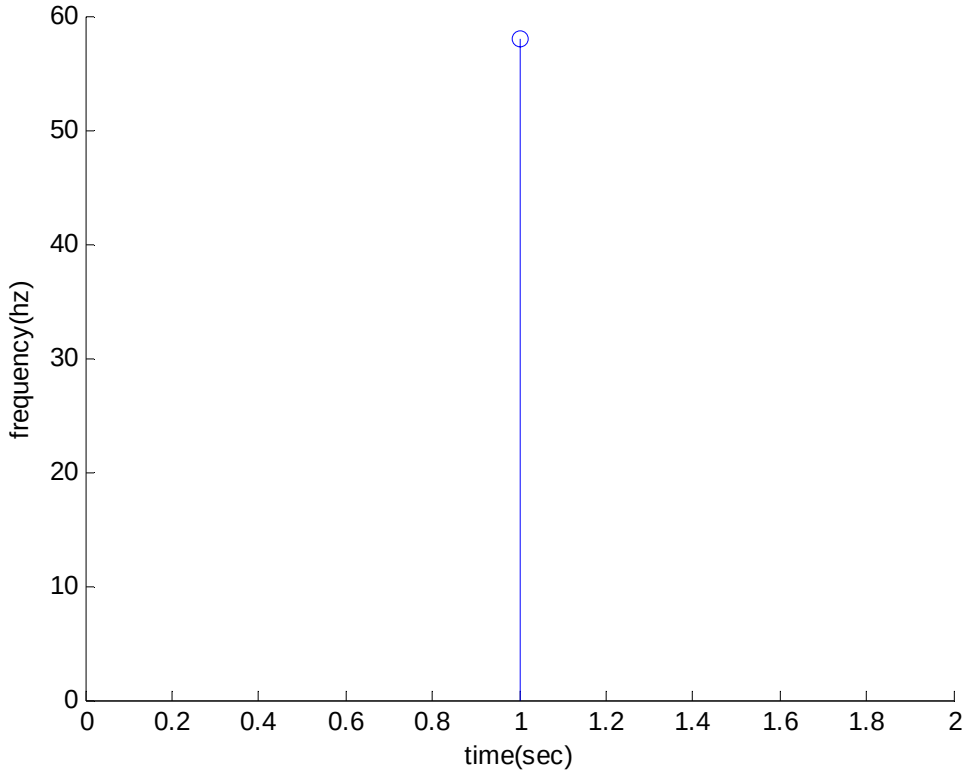

Figure 4.1.1: Estimated frequency with single harmonic using SDFT method. $SDFT_1$ **(m=1).**

4.2 Phasor estimation

From (4.1.26), it is observed that SDFT can provide exact frequency using $\hat{x}_r$, $\hat{x}_{r+1}$, $\hat{x}_{r+2}$, $\hat{x}_{r+3}$ and $\hat{x}_{r+4}$ in the presence of harmonics. Moreover, we can estimate phasor after getting exact "f " by the following equations:

$$A_r = a\hat{Z}_{r+1} - \hat{Z} / (a^2 - 1)(a^{1-m} - 1)(a^{1+m} - 1) ----(4.2.1).$$

$$X_1 = abs(A_r)N\sin(\pi\Delta f / 60N)/\sin(\pi\Delta f / 60).----(4.2.2).$$

$$\phi_1 = angle(A_r) - \pi / 60N(\Delta f(N-1)).----(4.2.3).$$

4.3 SDFT with multiple harmonics

It appears that SDFT can take integral order harmonics into consideration. To distinguish easily, SDFT means calculating frequency for $m=1$ and we add suffix to the others, for example $SDFT_3$ and $SDFT_{35}$ calculate frequency for $m=3$ and $m=3,5$, respectively. And here we offer the polynomial equation of $SDFT_3$ ($m=3$):

$$a^4 + p_3a^3 + p_2a^3 + p_1a + p_0 = 0.$$

Where

$$p_3 = -\hat{x}_{r+1} + \hat{x}_{r+3}/2\hat{x}_{r+2}, \qquad p_2 = -3/4,$$

$$p_1 = \hat{x}_{r+1} + \hat{x}_{r+3}/4\hat{x}_{r+2}, \qquad p_0 = \hat{x}_r + 2\hat{x}_{r+2} + \hat{x}_{r+4}/16\hat{x}_{r+2},$$

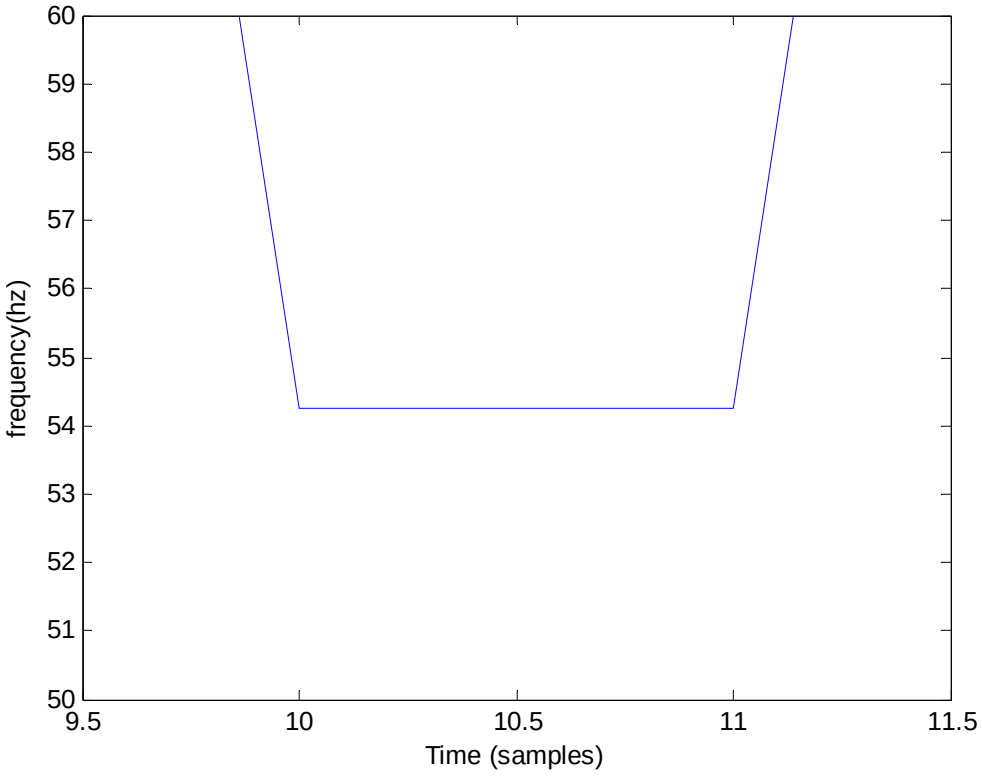

Figure 4.3.1: Estimated frequency of a multiple harmonic with SDFT method, $SDFT_3$ (m=3),

Actually, if we assume that $x(t) = X_1\cos(\omega t + \phi_1) + X_2\cos(m\omega t + \phi_2)$ from the beginning of development of the algorithm, we will derive a polynomial equation similar to (4.1.26) that provide exact frequency in the presence of nonintegral harmonic. We add suffix "n " to SDFT means that has taken nonintegral harmonics into consideration. Although we can take

all of the harmonics into consideration, we still need a digital filter to decay noise and high order harmonics. Since, in SDFT, the more harmonics taken into consideration, the more CPU time needed in computing. The advantages of digital filtering are no voltage drop, no temperature drift, no noise addition, and don't have any analog filter element features, like aging. Besides these, digital filter can be implemented in microprocessor-based equipment. These make us choose a digital filter to filter noise and high order harmonics. There are many digital filters that we can choose e.g., Hanning, Hamming and Blackman windows. In our simulations we will use the Blackman window for filtering.

4.4 simulation results

Simulation results presented in this section were all simulated from Matlab and showed a fair comparison to both the DFT method and Prony method. In Fig.4.4.1, we showed that SDFT could obtain an exact solution identical to the Prony method under frequency deviation in a pure sinusoidal waveform. Fig 4.4.1. also shows the performance of SDFT method and conventional DFT method. It is observed that conventional DFT method gives the wrong frequency calculations.

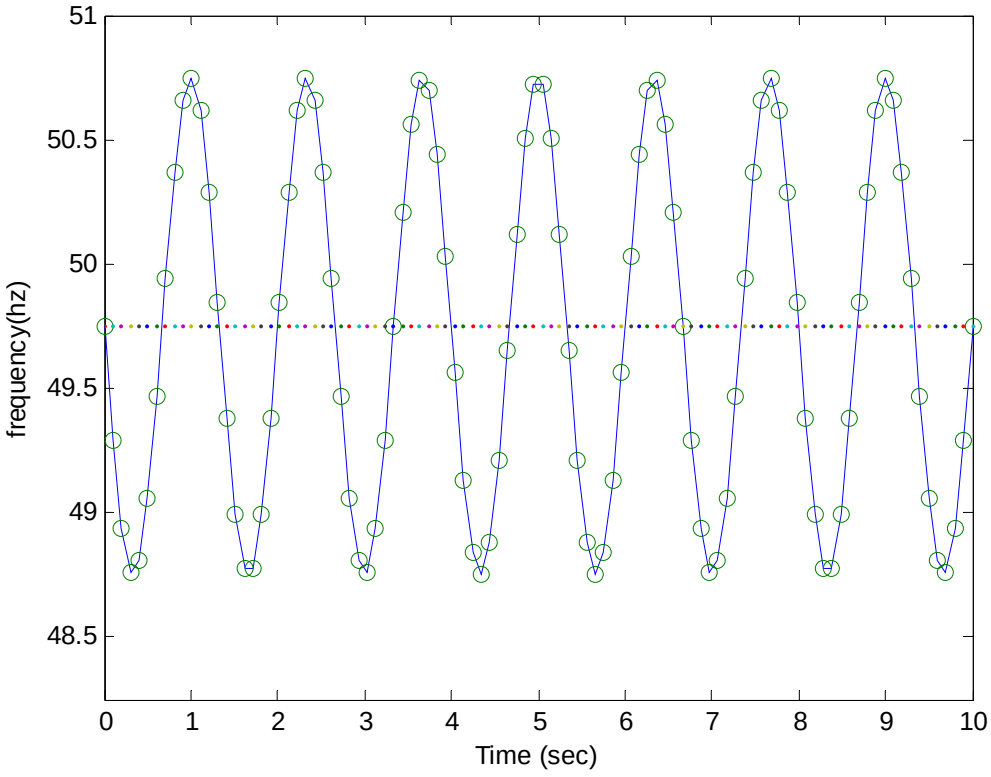

Figure 4.4.1: comparison of frequency calculations among DFT, Prony , SDFT and $SDFT_3$ [Test signal $x(t) = \cos(\omega t)$, f =51 Hz.

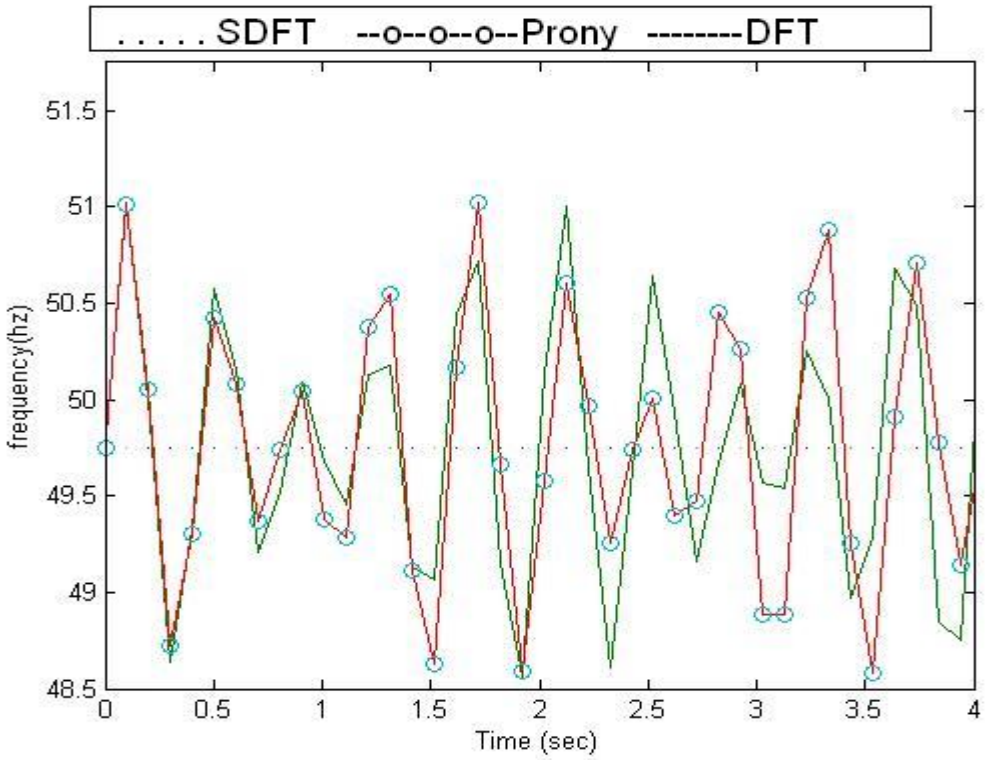

Figure 4.4.2: comparison of frequency calculations among DFT, Prony , SDFT and $SDFT_3$ **[Test signal** $x(t) = \cos(\omega t) + .05\cos(3\omega t) + .02\cos(5\omega t)$; **,** f **=50.5 Hz.**

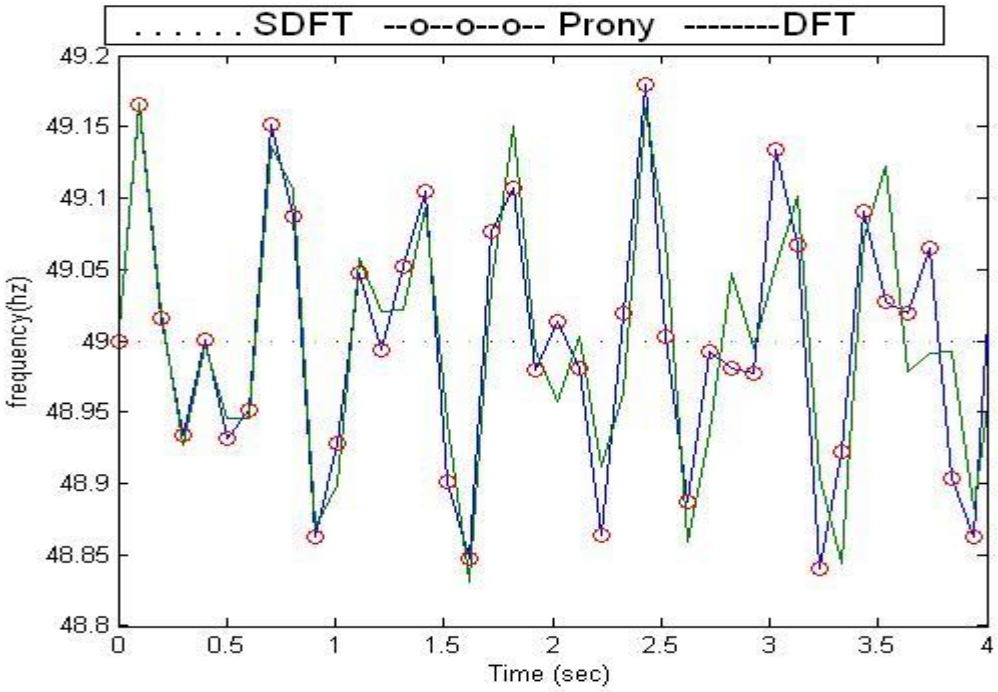

Figure 4.4.3: comparison of frequency calculations among DFT, Prony , SDFT and $SDFT_3$ **with Blackman window [Test signal** $x(t) = \cos(\omega t) + .05\cos(3\omega t) + .02\cos(5\omega t)$; f **=50.5 Hz.**

In Fig. 4.4.3, SDFT and SDFT3 are observed to obtain the exact solution. While the SDFT and Prony methods test the same signal without filtering, we find that Prony is worse than SDFT in the presence of harmonics, but if the test signal is filtered by a Blackman window (window size = 16) for estimation, we find that the SDFT and Prony methods have similar performance.

Chapter 5

DISCUSSION

Discussion:

The frequency is changed as a sine wave and 3rd, 5th harmonics is also added in test signal during 1 second. We can observe the errors of SDFT and Prony with Blackman window , and the errors of SDFT and SDFT without filter . Although SDFT and SDFT can resist the effect of the 3rd, 5th harmonics, the effect of frequency variation makes them get some small errors. We change 5th harmonic to a nonintegral harmonic, and of course SDFT has better performance than SDFT . However, this is a special case for SDFT . In fact, SDFT spends more time in computing than SDFT , and sometimes it has convergence problem when there are more than two harmonics in the signal. Anyway, from Fig. 5.1.1 we can conclude that SDFT-family algorithms (PRONY, SDFT and SDFT3) are better than DFT method and Prony method for frequency calculation.

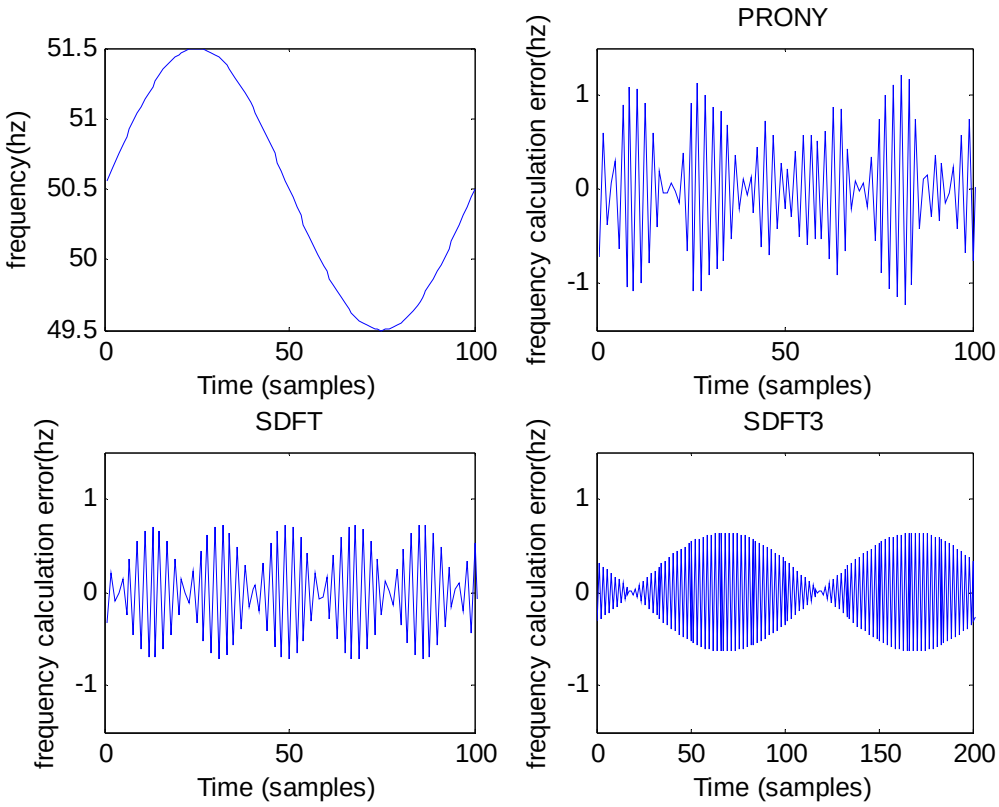

Figure 5.1.1: frequency variation of test signal ($x(t) = \cos(\omega t)$ f **=50+0.5** $\sin(2\pi t)$ **Hz), comparison of error of frequency calculations between Prony, SDFT and** $SDFT_3$**.**

By comparison of computation speed, Table I shows the AMD K6-200 CPU time of each method. There are 960 data per second computed by each method [the test signal is the same as in Fig. 3(a)] without a Blackman window to calculate the frequency, while adding a Blackman window will add 0.91 second to the computation. We find that SDFT is the fastest

method in these computations, even faster than DFT, because SDFT counts frequencies directly, but DFT has to count the phase first and then use the phase difference to count frequencies. The faster speed of SDFT over the Prony method is because recursion can be used in SDFT.

	Prony	DFT	SDFT	$SDFT_3$
Time (sec)	2.03	0.71	0.54	1.01

Table 5.1: computation time for different methods

Chapter 6

CONCLUSION & SCOPE FOR FUTURE WORK

6.1 Conclusions

In This work we came to know about The SDFT-family methods and demonstrate their performance. SDFT both keeps the advantages of DFT and also deals with the cause of frequency deviation errors, while taking harmonics into consideration. These aspects make SDFT a fast, accurate and harmonic-resisting method. But we do not suggest taking all the harmonics into consideration, since that would require too much computation time. Alternatively, using a smoothing window to decay the high order harmonics and just taking the low order harmonics into consideration will be more efficient and suitable for power systems under real-time demands.

6.2 Suggested future work

- The digital filters that we can choose e.g. Hanning, Hamming and Blackman window, can achieve the more efficient results in the presence of high order harmonics.
- The smoothing windows can be reduced the too much computation time.
- Stability study of the SDFT family.

Chapter 7

REFERENCES

References:

[1] P. J. Moore, R. D. Carranza, and A. T. Johns, "Model system tests on a new numeric method of power system frequency measurement," *IEEE Trans. on Power Delivery*, , Apr. 1996 vol. 11, no. 2, pp. 696–701.

[2] M. M. Begovic, P. M. Djuric, S. Dunlap, and A. G. Phadke, "Frequency tracking in power networks in the presence of harmonics," *IEEE Trans. on Power Delivery*, , Apr. 1993 vol. 8, no. 2, pp. 480–486.

[3] C. T. Nguyen and K. Srinivasan, "A new technique for rapid tracking of frequency deviations based on level crossings," *IEEE Trans. on Power Apparatus and Systems*, , Aug. 1984 vol. PAS-103, no. 8, pp. 2230–2236.

[4] I. Kamwa and R. Grondin, "Fast adaptive schemes for tracking voltage phasor and local frequency in power transmission and distribution systems," *IEEE Trans. on Power Delivery*, , Apr. 1992 vol. 7, no. 2, pp. 789–795.

[5] M. S. Sachdev and M. M. Giray, "A least error squares technique for determining power system frequency," *IEEE Trans. on Power Apparatus and Systems*, , Feb. 1985 vol. PAS-104, no. 2, pp. 437–443.

[6] M. M. Giray and M. S. Sachdev, "Off-nominal frequency measurements in electric power systems," *IEEE Trans. on Power Delivery*, , July 1989 vol. 4, no. 3, pp. 1573–1578.

[7] V. V. Terzija, M. B. Djuric, and B. D. Kovacevic, "Voltage phasor and local system frequency estimation using newton type algorithm," *IEEE Trans. on Power Delivery*, July 1994 vol. 9, no. 3, pp. 1368–1374.

[8] M. S. Sachdev, H. C. Wood, and N. G. Johnson, "Kalman filtering applied to power system measurements for relaying," *IEEE Trans. On Power Apparatus and System*, , Dec. 1985 vol. PAS-104, no. 12, pp. 3565–3573.

[9] A. A. Girgis and T. L. D.Hwang, "Optimal estimation of voltage phasors and frequency deviation using linear and nonlinear kalman filter: Theory and limitations," *IEEE Trans. on Power Apparatus and Systems*, Oct. 1984 vol. 103, no. 10, pp. 2943–2949.

[10] A. A. Girgis and W. L. Peterson, "Adaptive estimation of power system frequency deviation and its rate of change for calculating sudden power system overloads," *IEEE Trans. on Power Delivery*, , Apr. 1990 vol. 5, no. 2, pp. 585–594.

[11] T. Lobos and J. Rezmer, "Real-time determination of power system frequency," *IEEE Trans. on Instrumentation and Measurement*, Aug. 1997 vol. 46, no. 4, pp. 877–881,.

[12] A. G. Phadke, J. S. Thorp, and M. G. Adamiak, "A new measurement technique for tracking voltage phasors, local system frequency, and rat of change of frequency," *IEEE Trans. on Power Apparatus and Systems*, May 1983 vol. 102, no. 5, pp. 1025–1038,.

[13] Ph. Denys, C. Counan, L. Hossenlopp, and C. Holweck, "Measurement of voltage phase for the French future deffence plan against losses of synchronism," *IEEE Trans. on Power Delivery*, Jan. 1992 vol. 7, no. 1, pp. 62–69,.

[14] A. G. Phadke, M. Ibrahim, T. Hlibka, "Fundamental basis for Distance Relaying with Symmetrical Components", IEEE Trans. on PAS, March/April 1997 Vol. PAS-96, No.2, pp 635-646,.

[15] J. S. Thorp, A. G. Phadke, S. H. Horowitz, J. E. Beehler, "Limits to Impedance Relaying", IEEE Trans. on PAS, Vol. PAS-98, No.1, Jan/Feb 1979, pp 246-260.

[16] T. Lobos, "Non recursive methods for real-time determination of basic waveforms of voltages and currents," *IEE Proc.*, , Nov. 1989 vol. 136, pp. 347–351.

[17] K.-F. Eichhorn and T. Lobos, "Recursive real-time calculation of basic waveforms of signals," *IEE Proc.*, Nov. 1991 vol. 138, pp. 469–470,.

[18] B. Boashash, "Estimating and interpreting the instantaneous frequency of a signal: Part I: Fundamentals, Part II: Algorithms and applications," *Proc. IEEE*, Apr. 1992 vol. 80, pp. 520–568,.

[19] K.-F. Eichhorn, T. Lobos, and P. Ruczewski, "Constrained frequency domain algorithm for determination of parameters of fundamental sine wave of signals," *IEE Proc.*, Nov. 1993 vol. 140, pp. 477–480,.

[20] A. Cichocki and T. Lobos, "Artificial neural networks for real-time estimation of basic waveforms of voltages and currents," *IEEE Trans. Power Syst.*, May 1994. vol. 9, pp. 612–618,